Measurement of the Drell-Yan Absolute Cross-Section in pp and pd Collisions with a 120 GeV Proton Beam at Fermilab

Chatura Kuruppu[1], Stephen Pate[1]

[1]New Mexico State University, Las Cruces, NM 88003, USA

February 11, 2026

Abstract

This analysis note reports on the determination of pp and pd Drell-Yan absolute cross sections from data collected using the Roadset 67 trigger. We seek preliminary approval of these results for presentation in upcoming conferences. This work extends previous analyses by incorporating both Liquid Hydrogen (LH_2) and Liquid Deuterium (LD_2) target data. Furthermore, significant updates to the efficiency corrections have been implemented. The reconstruction efficiency is now calculated using a global curve based on the $D1$ occupancy variable, integrated over all kinematic bins, as demonstrated in DocDB 11427. Additionally, the hodoscope efficiency correction has been upgraded from a constant factor to a dimuon-level calculation using RoadIDs and paddle-specific efficiencies (DocDB 11467). In this work, we report the measurement of the double-differential Drell-Yan cross-sections, $\mathrm{d}^2\sigma/\mathrm{d}x_F\mathrm{d}M$, and compare the results with theoretical predictions from Quantum Chromodynamics (QCD).

This work was supported in part by US DOE grant DE-FG02-94ER40847.

Contents

1 Introduction **5**

2 Analysis Methodology **5**
- 2.1 Data and Monte Carlo Samples 5
- 2.2 Event Selection 6
- 2.3 Cross-Section Formalism 7

3 Acceptance and Efficiency Corrections **9**
- 3.1 Detector Acceptance Correction 9

4 Reconstruction Efficiency Correction **26**
- 4.1 Uncertainty Propagation 27

5 Hodoscope Efficiency Correction **29**

6 Total Efficiency Correction **34**

7 Determination of Corrected Yields **35**

8 Appendix: Event Selection Criteria (Chuck Cuts) **37**
- 8.1 Single Track Cuts 37
- 8.2 Dimuon Cuts 37
- 8.3 Occupancy and Topology Cuts 37

9 Appendix: Efficiency Plots **39**

10 Appendix: Table of Systematic Errors **40**

11 Appendix: Table of Cross-Section Values **44**

12 Appendix: Transverse Momentum Distributions **48**

List of Figures

1 Dimuon distributions after applying event selection criteria. . . . 8
2 Acceptance plots for $0.00 \leq x_F < 0.05$. . . . 10
3 Acceptance plots for $0.05 \leq x_F < 0.10$. . . . 11
4 Acceptance plots for $0.10 \leq x_F < 0.15$. . . . 12
5 Acceptance plots for $0.15 \leq x_F < 0.20$. . . . 13
6 Acceptance plots for $0.20 \leq x_F < 0.25$. . . . 14
7 Acceptance plots for $0.25 \leq x_F < 0.30$. . . . 15
8 Acceptance plots for $0.30 \leq x_F < 0.35$. . . . 16
9 Acceptance plots for $0.35 \leq x_F < 0.40$. . . . 17
10 Acceptance plots for $0.40 \leq x_F < 0.45$. . . . 18
11 Acceptance plots for $0.45 \leq x_F < 0.50$. . . . 19
12 Acceptance plots for $0.50 \leq x_F < 0.55$. . . . 20
13 Acceptance plots for $0.55 \leq x_F < 0.60$. . . . 21
14 Acceptance plots for $0.60 \leq x_F < 0.65$. . . . 22
15 Acceptance plots for $0.65 \leq x_F < 0.70$. . . . 23
16 Acceptance plots for $0.70 \leq x_F < 0.75$. . . . 24
17 Acceptance plots for $0.75 \leq x_F < 0.80$. . . . 25
18 Global Reconstruction Efficiency curve as a function of the $D1$ occupancy variable, integrated over all kinematic bins. . . . 26
19 Average Reconstruction Efficiencies calculated each kinematic bin with the propagated uncertainties. . . . 28
20 Hodoscope Paddle Efficiencies (Top Planes). . . . 29
20 Hodoscope Paddle Efficiencies (Bottom Planes) – Continued. . . . 30
21 Hodoscope Paddle hit distributions arranged by Plane (Rows 1-4), Top vs Bottom. 32
22 Average Hodoscope Efficiencies calculated each kinematic bin with the propagated uncertainties. . . . 33
23 Average total Efficiencies calculated each kinematic bin with the propagated uncertainties. . . . 34
24 Average efficiency correction for signal and final corrected yields. . . . 36

List of Tables

1 Single track selection criteria. 37
2 Dimuon kinematic and vertex selection criteria. 38
3 Occupancy and topological cuts. 38
4 Detailed Systematic Error calculation for Bins in x_F and Mass 40
5 Detailed cross-section calculation for Bins in x_F and Mass 44

1 Introduction

The Drell-Yan process, where a quark from one hadron annihilates with an antiquark from another to produce a lepton-antilepton pair ($q\bar{q} \to \ell^+\ell^-$), provides a clean and direct probe of the antiquark structure of nucleons. Over the past several decades, Drell-Yan experiments have been instrumental in mapping the parton distribution functions (PDFs) of the proton and other hadrons. However, most existing data are concentrated at small to moderate values of the parton momentum fraction, $x < 0.3$. The region of large x ($x > 0.3$) remains relatively unexplored, yet it is crucial for understanding phenomena such as the flavor asymmetry of the proton's light antiquark sea ($\bar{d}(x)/\bar{u}(x)$) and the fundamental mechanisms of non-perturbative QCD that govern hadron structure.

The SeaQuest experiment (E906) at Fermilab was designed specifically to explore this high-x frontier. By impinging a high-intensity 120 GeV proton beam from the Main Injector onto various fixed targets, including liquid hydrogen (LH_2) and liquid deuterium (LD_2), SeaQuest measures dimuon production in a kinematic region sensitive to antiquarks carrying a large fraction of the nucleon's momentum.

This analysis presents a measurement of the absolute double-differential Drell-Yan cross-section, binned in the dimuon invariant mass (M) and Feynman-x (x_F), using data collected with the LH_2 and LD_2 targets. The p+p collisions are primarily sensitive to the $\bar{u}$ distribution in the proton, while the p+d collisions provide information on the sum of $\bar{u}$ and $\bar{d}$. These results provide stringent new constraints on modern PDF parameterizations in the valence-dominated region.

The cross-section is presented in its scaling form, which, in the leading-order Drell-Yan model, is independent of the center-of-mass energy, $\sqrt{s}$:

$$M^3 \frac{\mathrm{d}^2\sigma}{\mathrm{d}M\mathrm{d}x_F} = f(\tau) \tag{1}$$

where $\tau = M^2/s$. The experimental determination of this quantity requires a precise understanding of the integrated luminosity, detector acceptance, and reconstruction efficiencies, which are detailed in the subsequent sections of this document.

2 Analysis Methodology

The extraction of the Drell-Yan cross-section from the raw data involves several distinct steps: selecting candidate dimuon events, subtracting backgrounds, calculating the integrated luminosity, and correcting for detector- and reconstruction-related inefficiencies.

2.1 Data and Monte Carlo Samples

This analysis utilizes the "Roadset 67" dataset collected by the SeaQuest experiment. The primary data files for the liquid hydrogen (LH_2) target and the corresponding empty "flask" target runs are saved in:

`/seaquest/users/apun/e906_projects/rs67_merged_files/`

- **Data (LH_2 Target):** `merged_RS67_3089LH2.root`
- **Data (LD_2 Target):** `merged_RS67_3089LD2.root`
- **Background (Empty Flask):** `merged_RS67_3089Flask.root`

To properly correct for detector performance, we calculate the hodoscope and reconstruction efficiency corrections at the dimuon level. The above ROOT files were modified by adding the following variables to each event:

- `recoeff`: reconstruction efficiency correction
- `recoeff_error`: propagated uncertainty of the reconstruction efficiency correction
- `hodoeff`: hodoscope efficiency correction
- `hodoeff_error`: propagated uncertainty of the hodoscope efficiency correction

The updated datasets containing these variables are saved in the following locations:

- `/seaquest/users/ckuruppu/rootfiles/rs67/merged_RS67_3089_LH2_recoeff_hodoeff.root`
- `/seaquest/users/ckuruppu/rootfiles/rs67/merged_RS67_3089_LD2_recoeff_hodoeff.root`
- `/seaquest/users/ckuruppu/rootfiles/rs67/merged_RS67_3089_Flask_recoeff_hodoeff.root`

The empty flask data are crucial for subtracting contributions from beam interactions with the target vessel walls and other upstream material.

To correct for detector acceptance and reconstruction efficiencies, extensive Monte Carlo (MC) simulations were employed. The simulations model the Drell-Yan process and propagate the resulting muons through a Geant4-based model of the SeaQuest spectrometer. The primary MC files used are:

- **Acceptance Study:** Drell-Yan events were generated over a 4π solid angle ("thrown") and also processed through the full detector simulation and reconstruction chain ("accepted"). This study uses the `*_M027_S001_*` series of files saved in:

  `/seaquest/users/chleung/pT_ReWeight/`

  - `mc_drellyan_LH2_M027_S001_4pi_pTxFweight_v2.root`
  - `mc_drellyan_LH2_M027_S001_clean_occ_pTxFweight_v2.root`
  - `mc_drellyan_LH2_M027_S001_messy_occ_pTxFweight_v2.root`
  - `mc_drellyan_LD2_M027_S001_4pi_pTxFweight_v2.root`
  - `mc_drellyan_LD2_M027_S001_clean_occ_pTxFweight_v2.root`
  - `mc_drellyan_LD2_M027_S001_messy_occ_pTxFweight_v2.root`

- **Efficiency Study:** To model the effect of high detector occupancy on track reconstruction, simulated events were processed with ("messy") and without ("clean") the overlay of random background hits from experimental data. This study uses the `*_M027_S001_*` series of files also saved in the same location.

All MC samples are weighted on an event-by-event basis to match the transverse momentum (p_T) distribution observed in the data.

2.2 Event Selection

A multi-tiered set of selection criteria is applied to isolate high-quality Drell-Yan dimuon events from the large background of other processes.

- **Data Quality:** Only data from "good spills," as identified by standard run quality monitoring, are included in the analysis. A physics trigger condition (`MATRIX1 == 1`) is required, selecting events consistent with the passage of two muons through the spectrometer.

- **Track and Dimuon Quality:** A set of stringent cuts, developed by the collaboration and referred to as "Chuck cuts," are applied to ensure well-reconstructed positive and negative muon tracks that form a high-quality common vertex. These cuts impose requirements on track χ^2, momentum, number of hits, and fiducial volume. The full details of these cuts are provided in Appendix 8.
- **Kinematic Selection:** The analysis focuses on the high-mass continuum, away from the charmonium resonances ($J/\psi, \psi'$). A cut of $M_{\mu\mu} > 4.2$ GeV is applied. The analysis is restricted to the kinematic range $0 < x_F < 0.8$.

After applying the event selection criteria mentioned in the Appendix, the total and mix yields for the LH_2, LD_2, and Empty Flask targets in each kinematic bin are extracted. The distributions are shown in Figure 1.

2.3 Cross-Section Formalism

The double-differential cross-section in a given kinematic bin $(\Delta M, \Delta x_F)$ is calculated as (refer DocDB 11445-V3):

$$\frac{\mathrm{d}^2\sigma}{\mathrm{d}M\mathrm{d}x_F} = \frac{1}{\epsilon_{\text{acc}}\Delta M \Delta x_F}\left[\frac{Y^{\text{LH2}}_{\text{total}} - Y^{\text{LH2}}_{\text{mixed}}}{\langle\epsilon^{\text{LH2}}_{\text{signal}}\rangle} - \frac{I_{\text{LH2}}}{I_{\text{flask}}}\left(\frac{Y^{\text{flask}}_{\text{total}} - Y^{\text{flask}}_{\text{mixed}}}{\langle\epsilon^{\text{flask}}_{\text{signal}}\rangle}\right)\right] \tag{2}$$

where:

- $Y^{\text{LH2}}_{\text{total}}$ is the total LH2 target dimuon yield after the event selection criteria.
- $Y^{\text{LH2}}_{\text{mixed}}$ is the estimated mixed background yield from mixed events for the LH2 target.
- $Y^{\text{flask}}_{\text{total}}$ is the total flask target dimuon yield after the event selection criteria.
- $Y^{\text{flask}}_{\text{mixed}}$ is the estimated mixed background yield from mixed events for the flask target.
- $\langle\epsilon^{\text{LH2}}_{\text{signal}}\rangle$ is the average signal efficiency correction for the LH2 target dimuons.
- $\langle\epsilon^{\text{flask}}_{\text{signal}}\rangle$ is the average signal efficiency correction for the flask target dimuons.
- $\mathcal{L}$ is the integrated luminosity for the dataset.

The average signal efficiency correction can be calculated as:

$$\langle\epsilon_{\text{signal}}\rangle = \frac{1}{Y_{\text{total}} - Y_{\text{mixed}}}\left[\langle\epsilon_{\text{total}\text{total}} - \langle\epsilon_{\text{mixed}\text{mixed}}\right] \tag{3}$$

where:

- $\langle\epsilon_{\text{total}}\rangle$ is the average total efficiency correction for the total yield.
- $\langle\epsilon_{\text{mixed}}\rangle$ is the average mixed efficiency correction for the mixed background yield.

as explained in DocDB 11448-V2.

In each case, efficiency correction of the i^{th} dimuon is defined as:

$$\epsilon^i = \epsilon^i_{\text{recon}} \cdot \epsilon^i_{\text{hodo}} \tag{4}$$

where $\epsilon^i_{\text{recon}}$ is the reconstruction efficiency for the i^{th} dimuon and ϵ^i_{hodo} is the hodoscope efficiency for the i^{th} dimuon. The calculation of these efficiency corrections is detailed in the following sections.

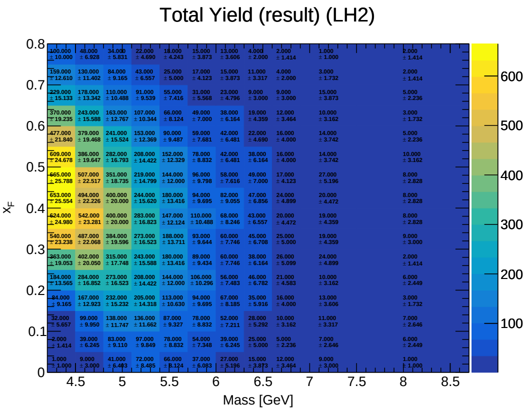

(a) LH2 total dimuon yield

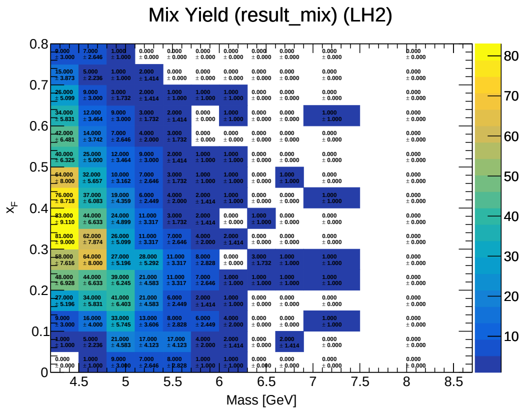

(b) LH2 mix dimuon yield

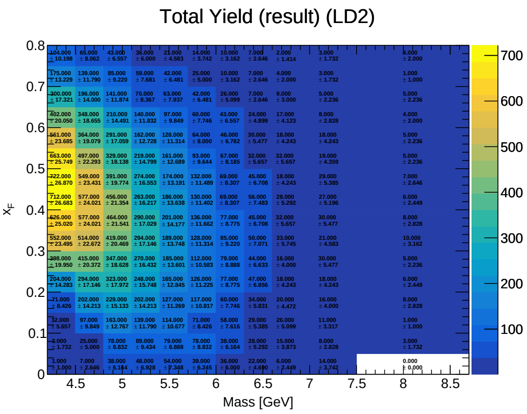

(c) Total LD2 dimuon yield

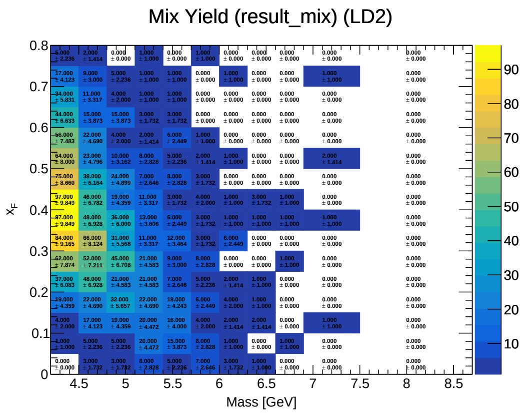

(d) LD2 mix dimuon yield

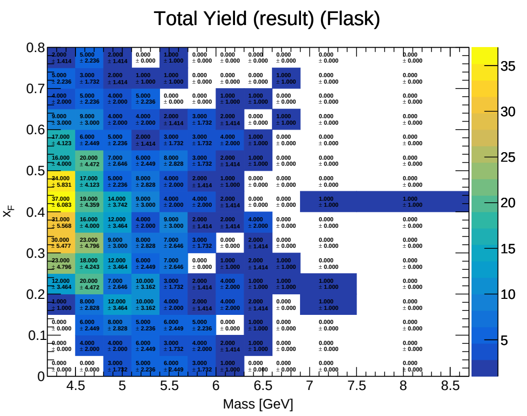

(e) Total Flask dimuon yield

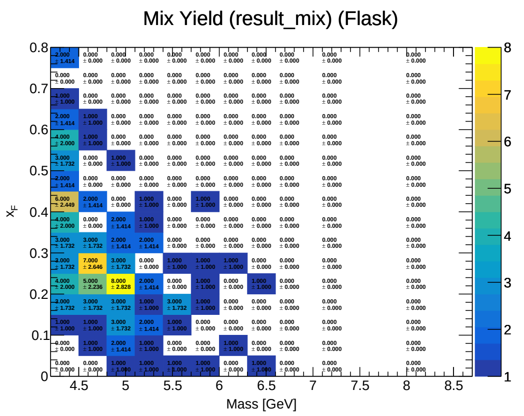

(f) Flask mix dimuon yield

Figure 1: Dimuon distributions after applying event selection criteria.

The integrated luminosity, $\mathcal{L}$, is given by the product of the total number of protons incident on the target and the number of target nuclei per unit area:

$$\mathcal{L} = N_{\text{incident}} \cdot \frac{N_A \rho L}{A} \cdot f_{\text{atten}} \tag{5}$$

Here, N_{incident} is the number of protons on target, N_A is Avogadro's number, ρ is the target density, L is the target length, A is the molar mass, and f_{atten} is a correction factor for beam attenuation within the thick target. For the $L = 50.8$ cm long LH_2 target, with a density of

$\rho_H = 0.0708$ g/cm^3, the target thickness is 3.5966 g/cm^2 with a beam attenuation factor of 0.966. Also, ϵ_{acc} is the geometric and kinematic acceptance of the spectrometer.

3 Acceptance and Efficiency Corrections

3.1 Detector Acceptance Correction

The SeaQuest spectrometer has a finite geometric acceptance, which limits the fraction of produced dimuon events that can be detected. This acceptance depends strongly on the event kinematics, primarily the dimuon invariant mass (M) and Feynman-x (x_F). The acceptance correction factor is determined using MC simulations.

The acceptance, $A(M, x_F)$, is defined as the ratio of the number of simulated events that are successfully reconstructed and pass all analysis cuts (N_{reco}) to the total number of events generated in a given kinematic bin (N_{gen}):

$$\text{Acceptance (A)} = \frac{N_{\text{reco}}}{N_{\text{gen}}} \tag{6}$$

This calculation is performed in bins of M and x_F. The kinematic binning used for this study is defined by the following edges:

- x_F **Edges**: $\{0, 0.05, 0.1, \ldots, 0.8\}$ (16 bins)
- **Mass Edges (GeV/c^2)**: $\{4.2, 4.5, 4.8, 5.1, 5.4, 5.7, 6, 6.3, 6.6, 6.9, 7.5, 8.7\}$ (11 bins)

The following pages show the calculated acceptance as a function of mass for each of the 16 x_F bins. The plots show the acceptance for the LH_2 and LD_2 targets, their combined average, and their ratio. The ratio is close to unity across the kinematic range, indicating that target-dependent effects on the acceptance are small. In this case, we compare newly calculated acceptance corrections to the existing acceptance calculations saved in Shivangi's file:

`./shivangi/work/analysis/R008/diffCross/v42/5770/looseCut/final/acceptance_h.root`

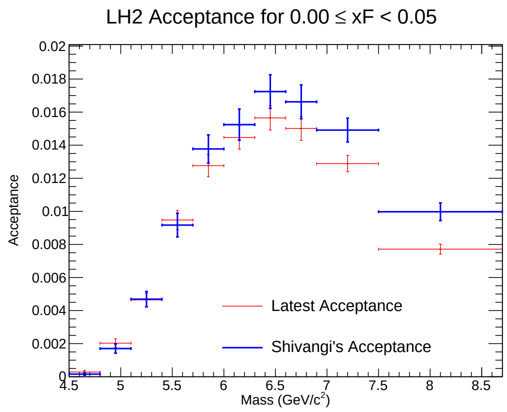

(a) Acceptance for LH2

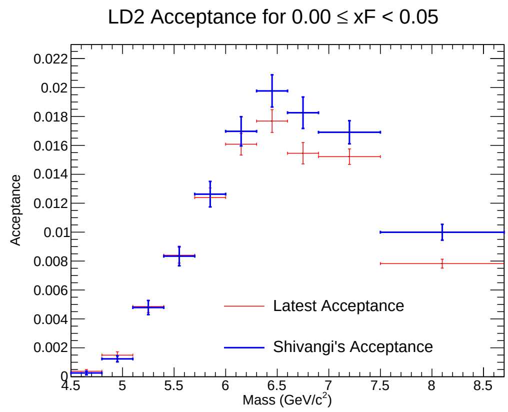

(b) Acceptance for LD2

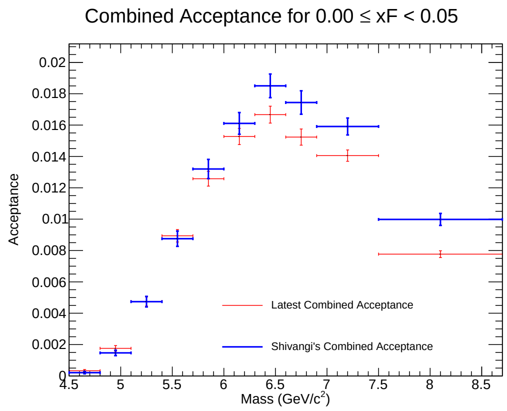

(c) Combined Acceptance

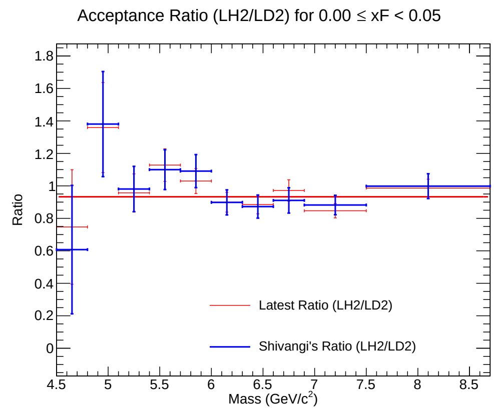

(d) Acceptance Ratio (LH2/LD2)

Figure 2: Acceptance plots for $0.00 \leq x_F < 0.05$.

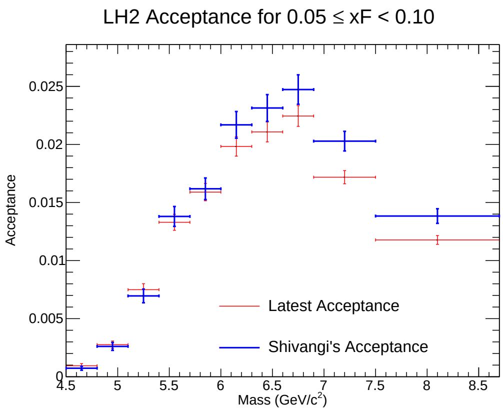

(a) Acceptance for LH2

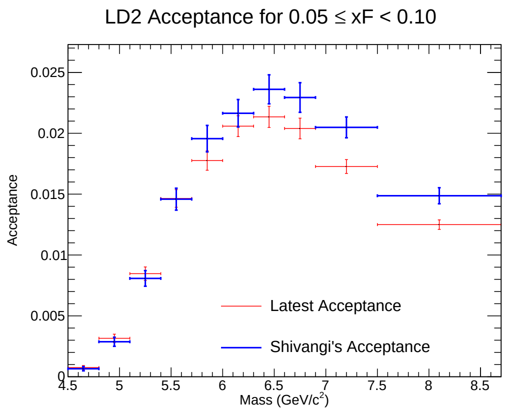

(b) Acceptance for LD2

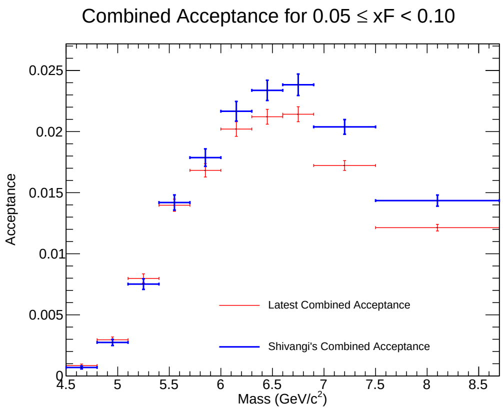

(c) Combined Acceptance

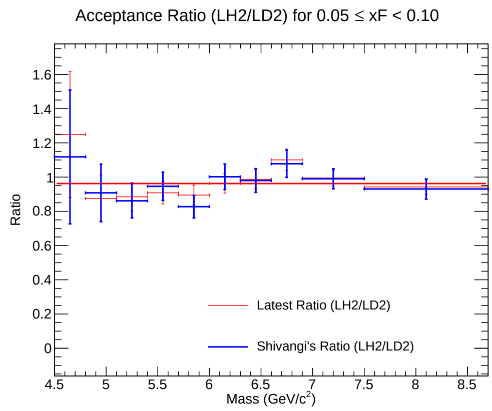

(d) Acceptance Ratio (LH2/LD2)

Figure 3: Acceptance plots for $0.05 \leq x_F < 0.10$.

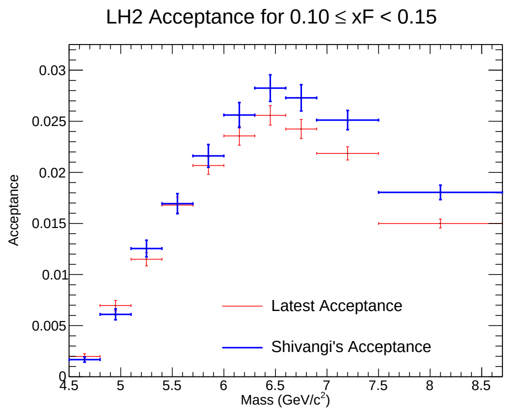

(a) Acceptance for LH2

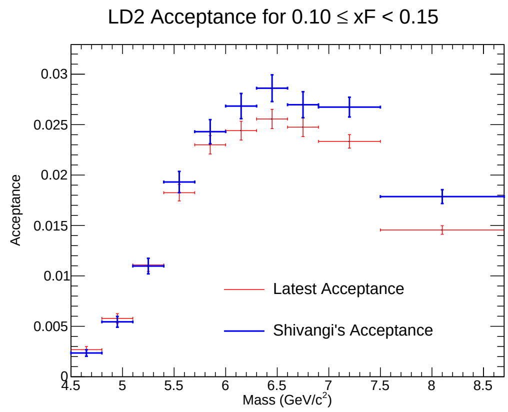

(b) Acceptance for LD2

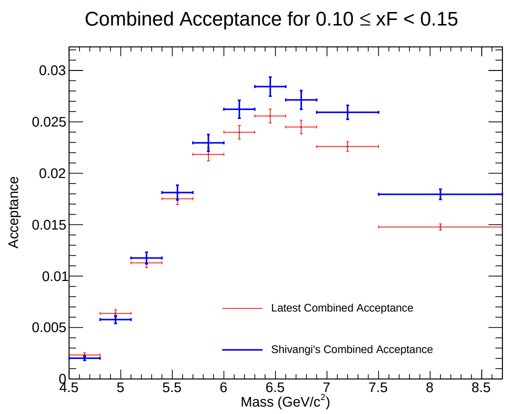

(c) Combined Acceptance

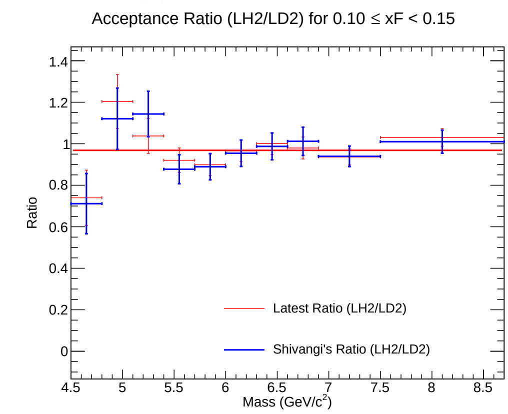

(d) Acceptance Ratio (LH2/LD2)

Figure 4: Acceptance plots for $0.10 \leq x_F < 0.15$.

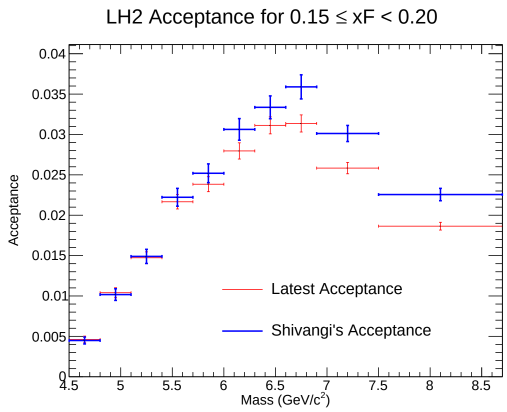

(a) Acceptance for LH2

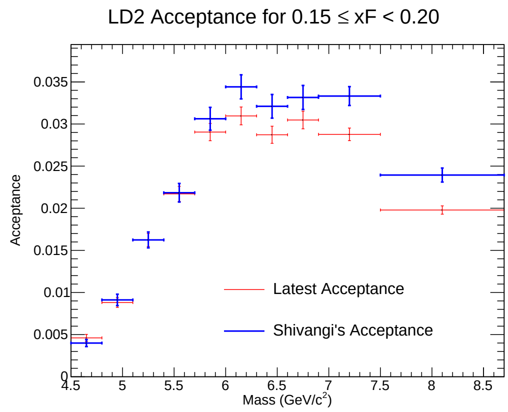

(b) Acceptance for LD2

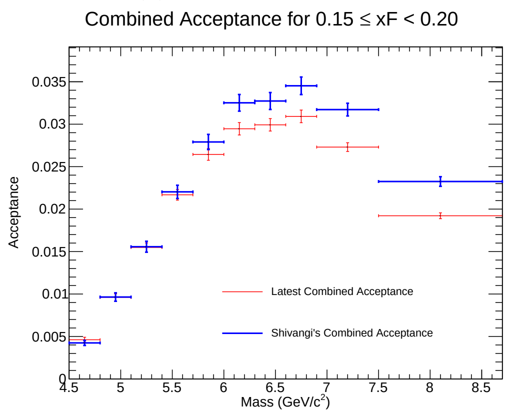

(c) Combined Acceptance

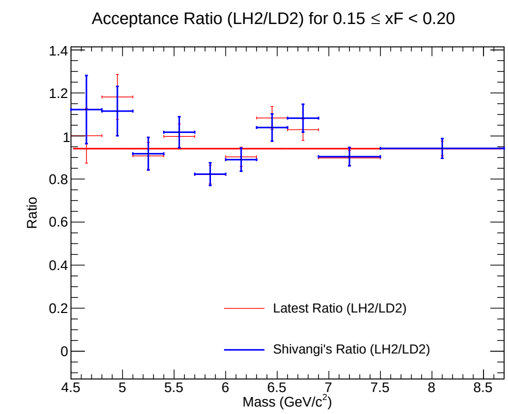

(d) Acceptance Ratio (LH2/LD2)

Figure 5: Acceptance plots for $0.15 \leq x_F < 0.20$.

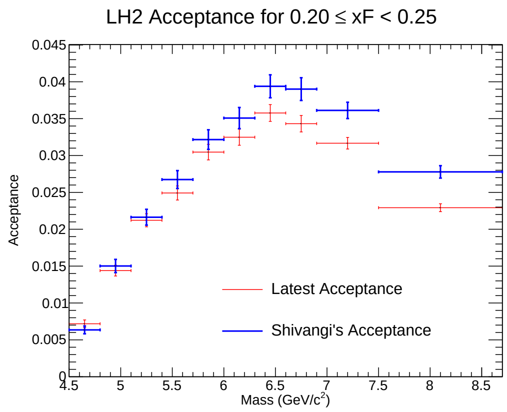

(a) Acceptance for LH2

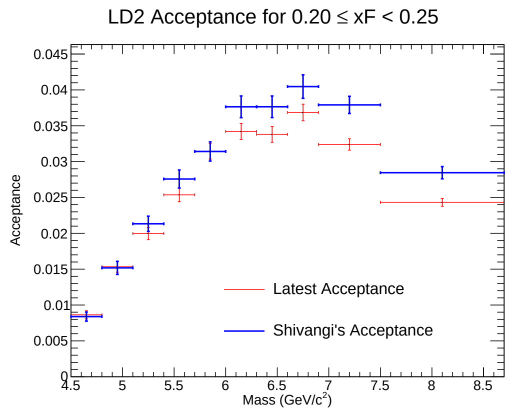

(b) Acceptance for LD2

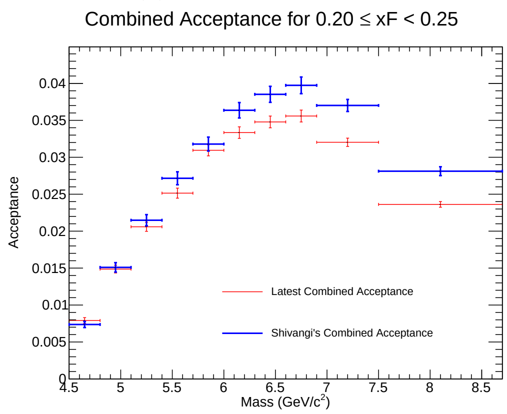

(c) Combined Acceptance

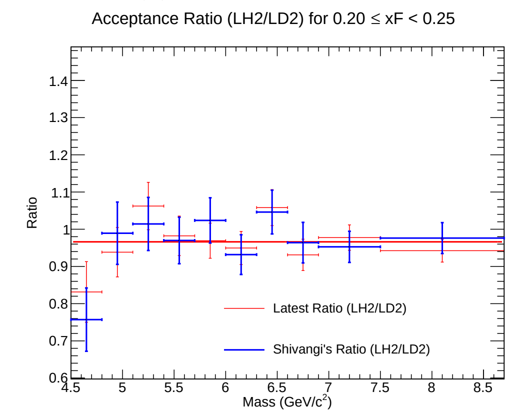

(d) Acceptance Ratio (LH2/LD2)

Figure 6: Acceptance plots for $0.20 \leq x_F < 0.25$.

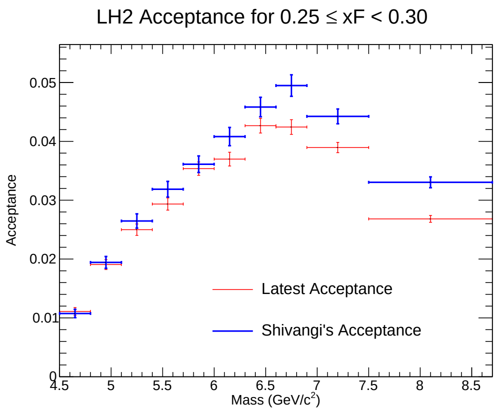

(a) Acceptance for LH2

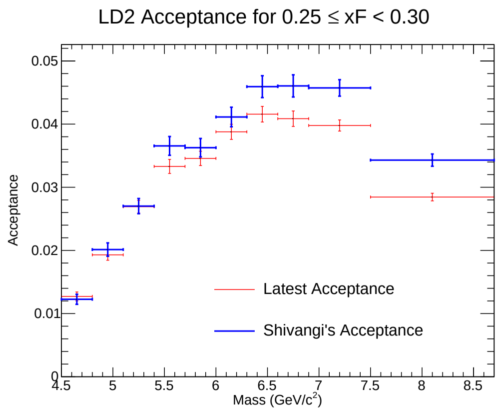

(b) Acceptance for LD2

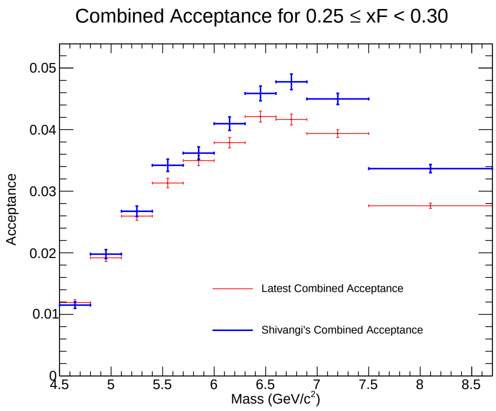

(c) Combined Acceptance

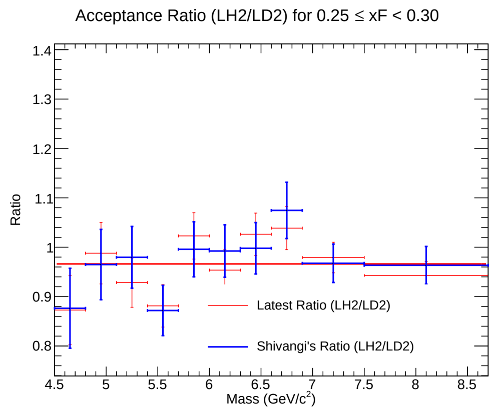

(d) Acceptance Ratio (LH2/LD2)

Figure 7: Acceptance plots for $0.25 \leq x_F < 0.30$.

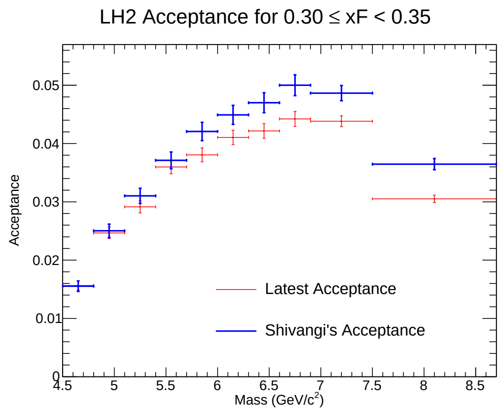

(a) Acceptance for LH2

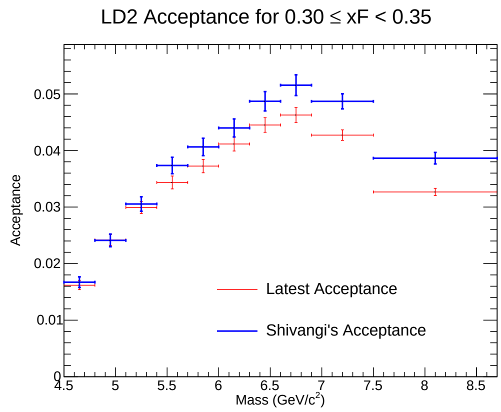

(b) Acceptance for LD2

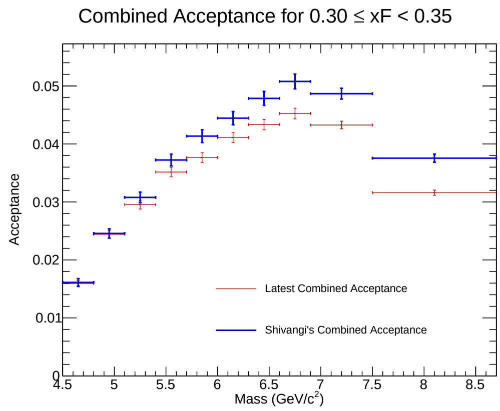

(c) Combined Acceptance

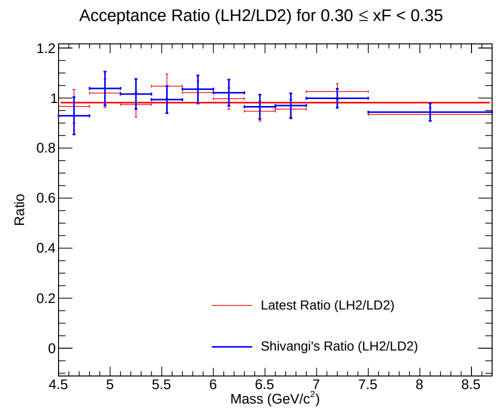

(d) Acceptance Ratio (LH2/LD2)

Figure 8: Acceptance plots for $0.30 \leq x_F < 0.35$.

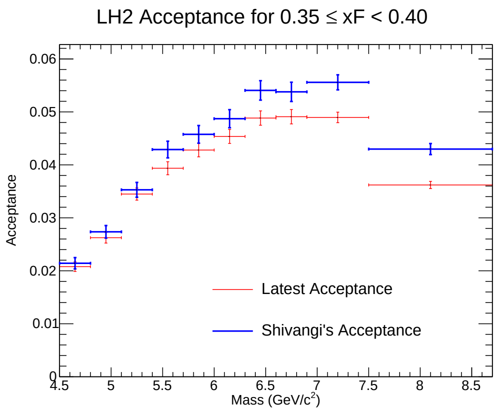

(a) Acceptance for LH2

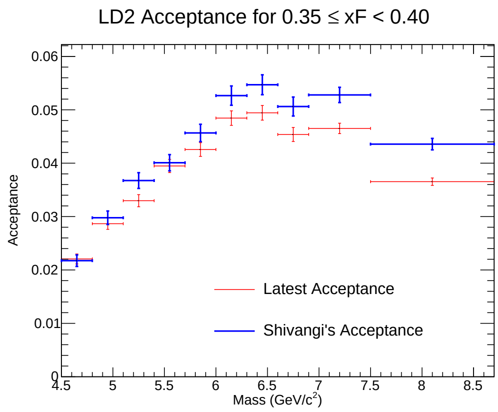

(b) Acceptance for LD2

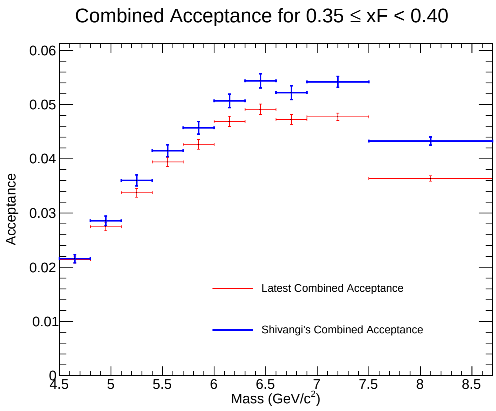

(c) Combined Acceptance

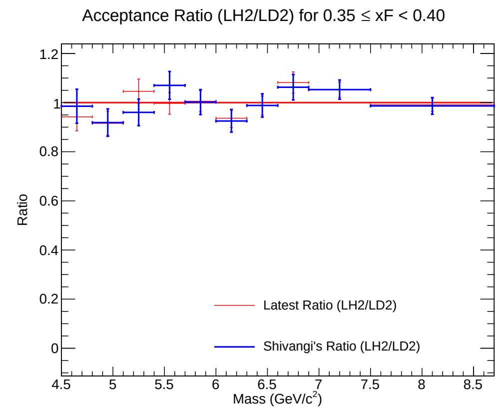

(d) Acceptance Ratio (LH2/LD2)

Figure 9: Acceptance plots for $0.35 \leq x_F < 0.40$.

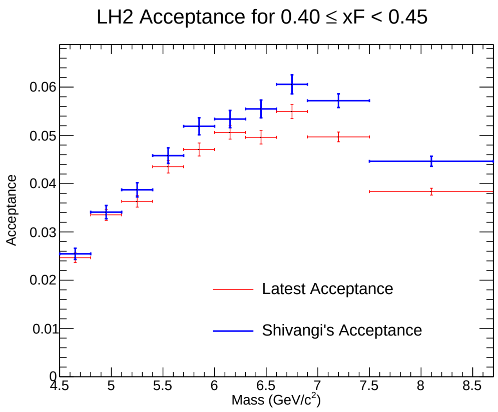

(a) Acceptance for LH2

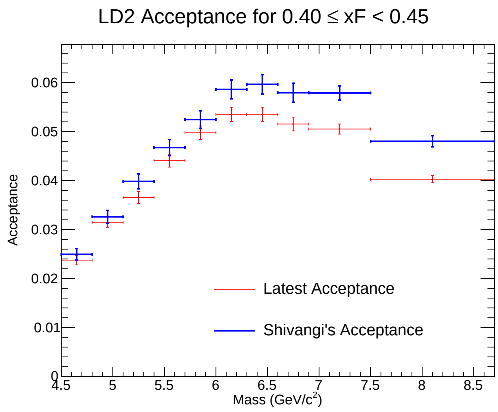

(b) Acceptance for LD2

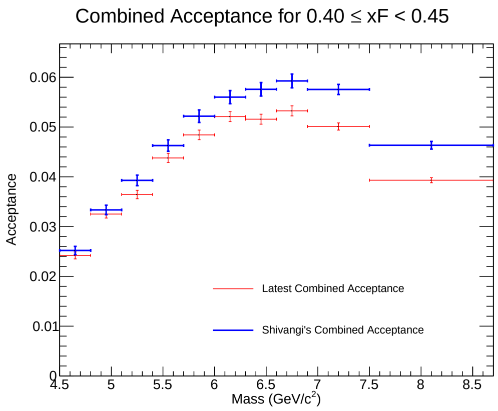

(c) Combined Acceptance

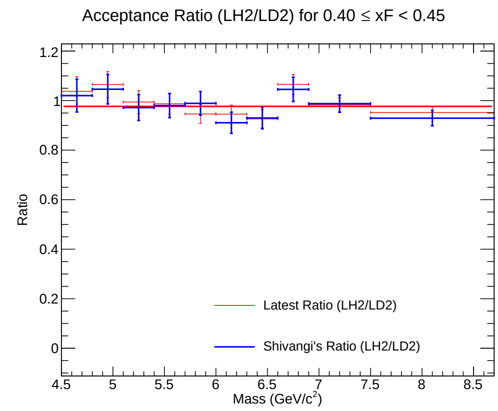

(d) Acceptance Ratio (LH2/LD2)

Figure 10: Acceptance plots for $0.40 \leq x_F < 0.45$.

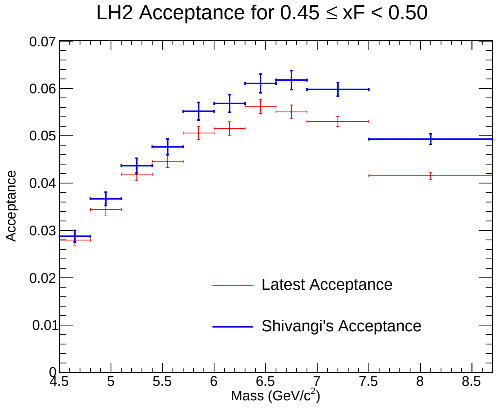

(a) Acceptance for LH2

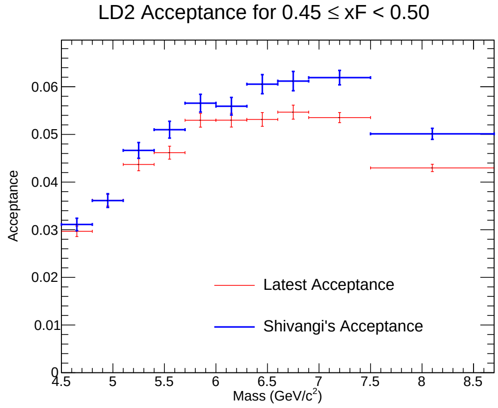

(b) Acceptance for LD2

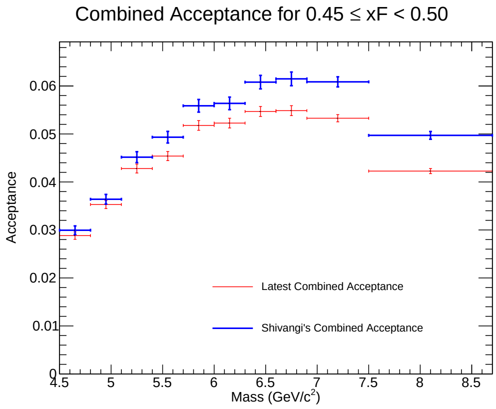

(c) Combined Acceptance

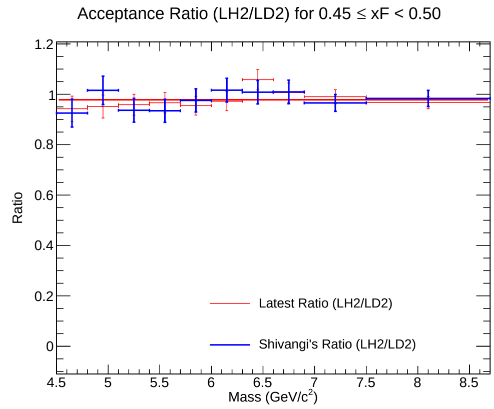

(d) Acceptance Ratio (LH2/LD2)

Figure 11: Acceptance plots for $0.45 \leq x_F < 0.50$.

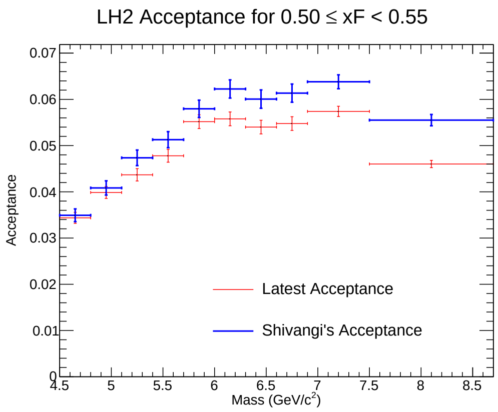

(a) Acceptance for LH2

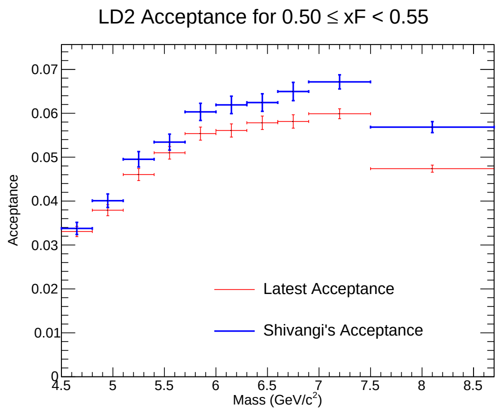

(b) Acceptance for LD2

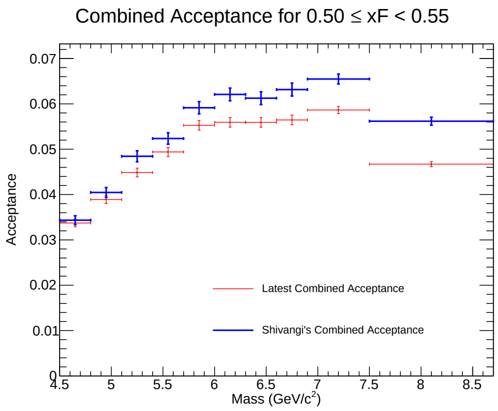

(c) Combined Acceptance

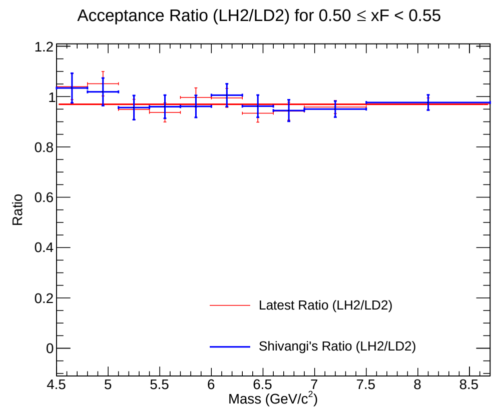

(d) Acceptance Ratio (LH2/LD2)

Figure 12: Acceptance plots for $0.50 \leq x_F < 0.55$.

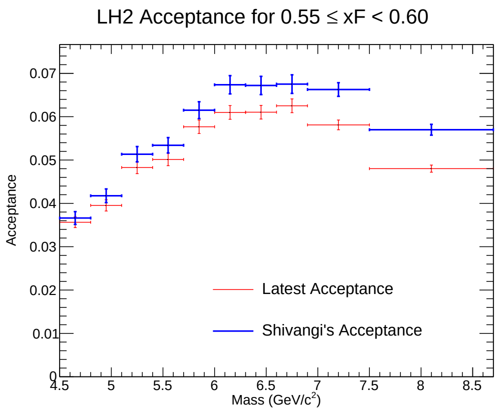

(a) Acceptance for LH2

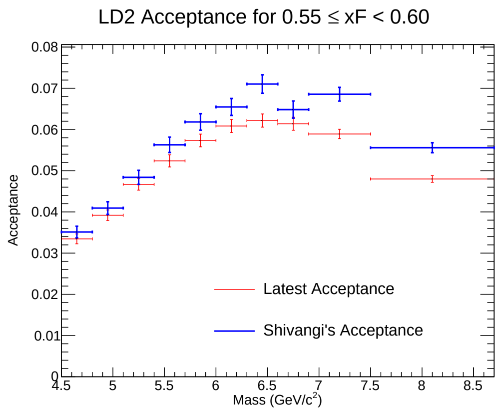

(b) Acceptance for LD2

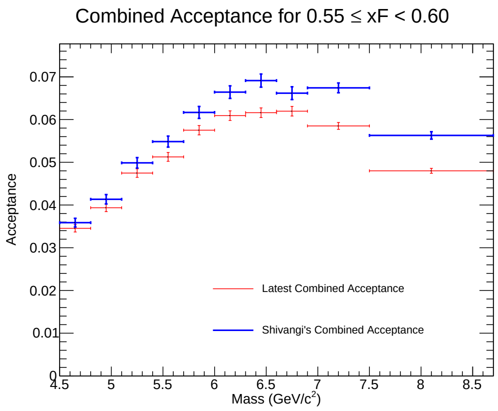

(c) Combined Acceptance

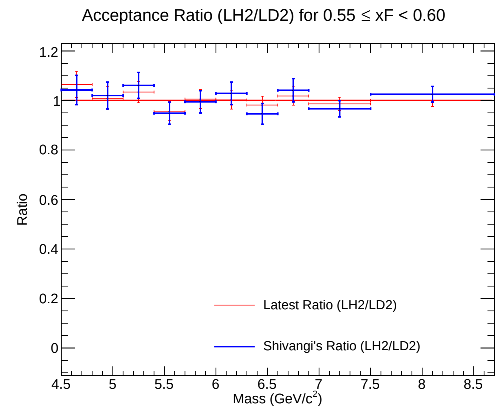

(d) Acceptance Ratio (LH2/LD2)

Figure 13: Acceptance plots for $0.55 \leq x_F < 0.60$.

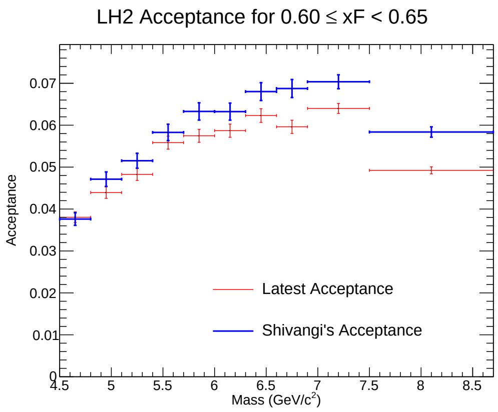

(a) Acceptance for LH2

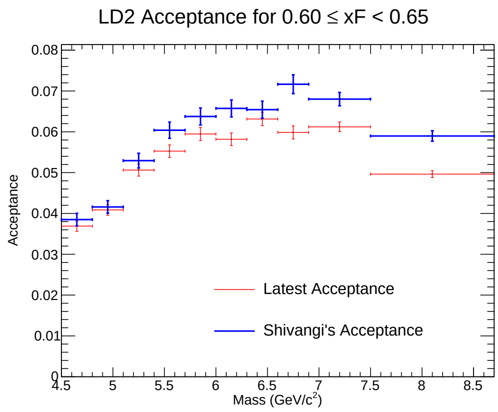

(b) Acceptance for LD2

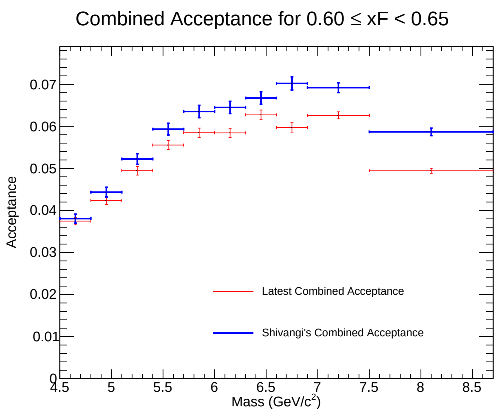

(c) Combined Acceptance

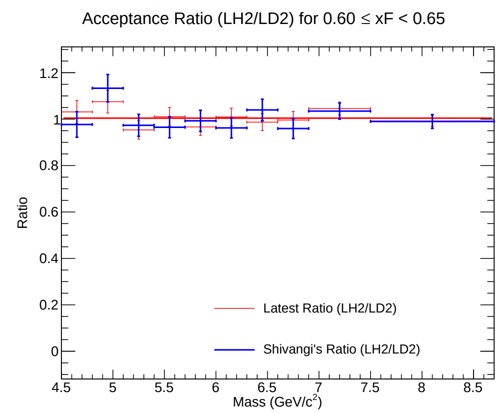

(d) Acceptance Ratio (LH2/LD2)

Figure 14: Acceptance plots for $0.60 \leq x_F < 0.65$.

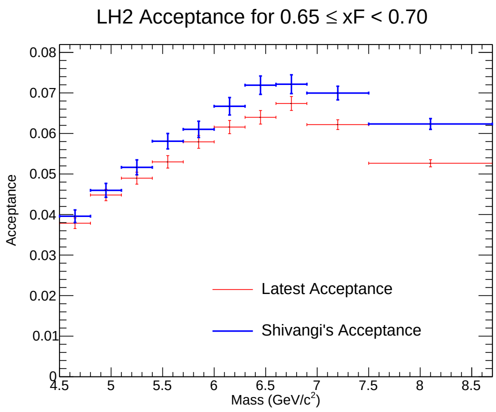

(a) Acceptance for LH2

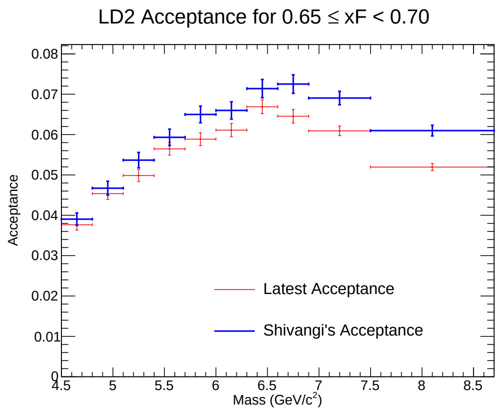

(b) Acceptance for LD2

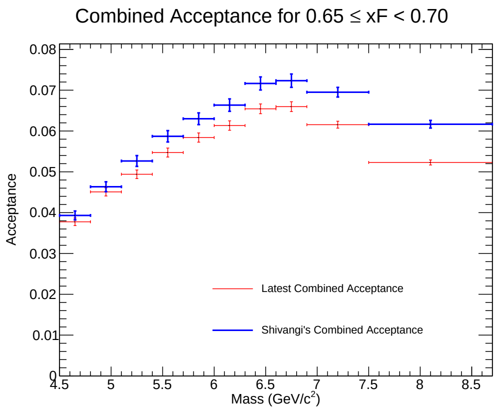

(c) Combined Acceptance

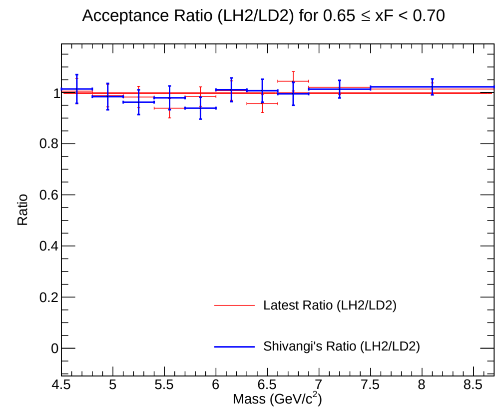

(d) Acceptance Ratio (LH2/LD2)

Figure 15: Acceptance plots for $0.65 \leq x_F < 0.70$.

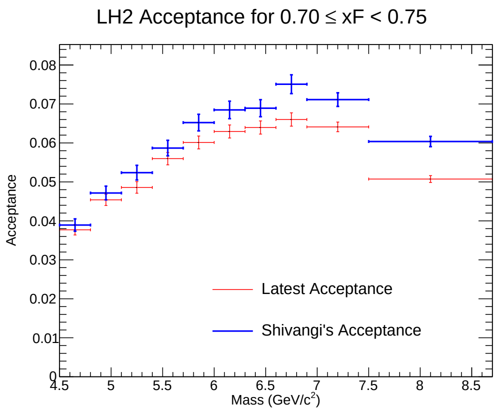

(a) Acceptance for LH2

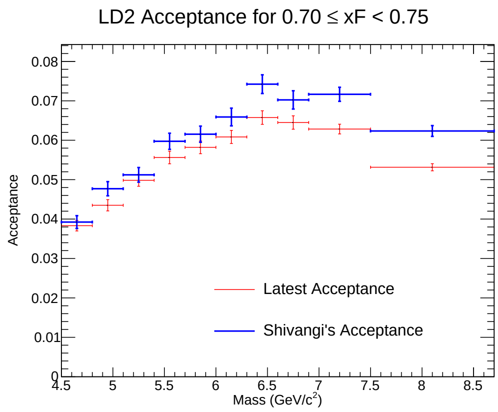

(b) Acceptance for LD2

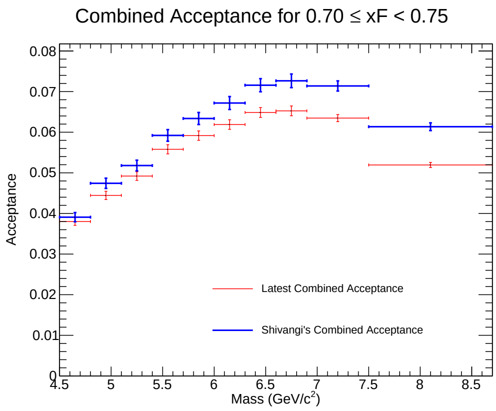

(c) Combined Acceptance

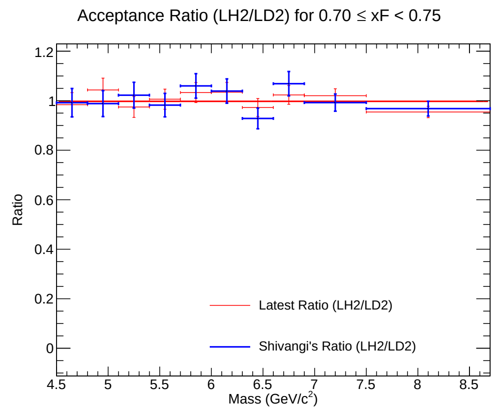

(d) Acceptance Ratio (LH2/LD2)

Figure 16: Acceptance plots for $0.70 \leq x_F < 0.75$.

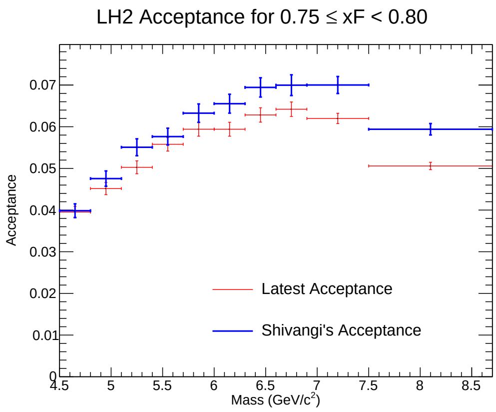

(a) Acceptance for LH2

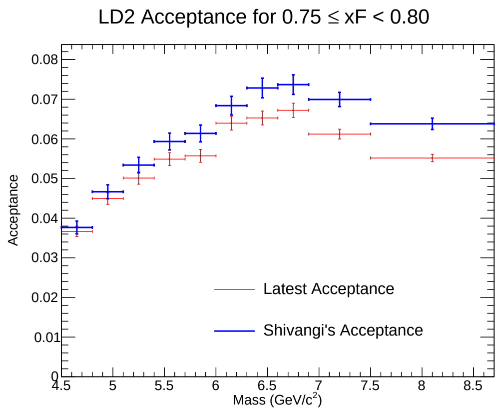

(b) Acceptance for LD2

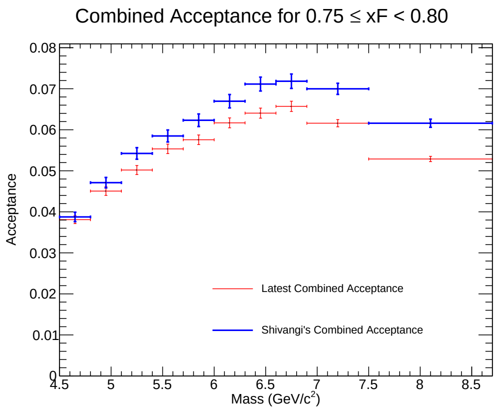

(c) Combined Acceptance

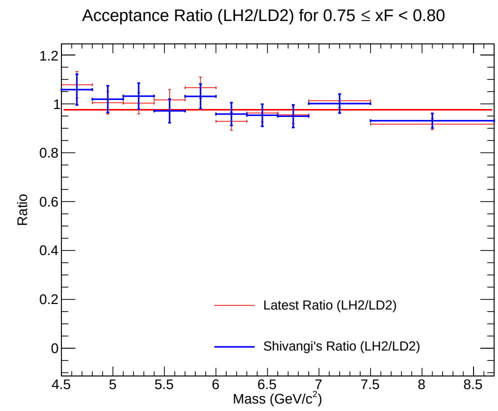

(d) Acceptance Ratio (LH2/LD2)

Figure 17: Acceptance plots for $0.75 \leq x_F < 0.80$.

4 Reconstruction Efficiency Correction

The track-finding algorithm ("kTracker") has an efficiency that depends on the detector occupancy; the number of hits in the detector during an event. This efficiency is studied using "clean" MC simulations (signal only) and "messy" MC simulations (signal with background hits overlaid). The reconstruction efficiency, ϵ_{recon}, is defined as the ratio of events found in the messy sample to those in the clean sample, as a function of an occupancy-related variable (e.g., D2, the number of hits in Drift Chamber Station 2).

$$\epsilon_{\text{recon}}(\text{D1}) = \frac{N_{\text{reco}}^{\text{messy}}(\text{D1})}{N_{\text{reco}}^{\text{clean}}(\text{D1})} \tag{7}$$

We have updated the reconstruction efficiency calculation compared to previous reconstruction efficiency calculation. Previously, reconstruction efficiency was calculated by creating curves in each kinematic bin using the $D2$ occupancy variable. However, it has been demonstrated that there is little correlation between reconstruction efficiency and different kinematic bins (DocDB 11427). Therefore, we utilize a **global reconstruction efficiency curve**, defined with efficiency on the y-axis and the $D1$ **occupancy variable** on the x-axis, integrated over all kinematic bins.

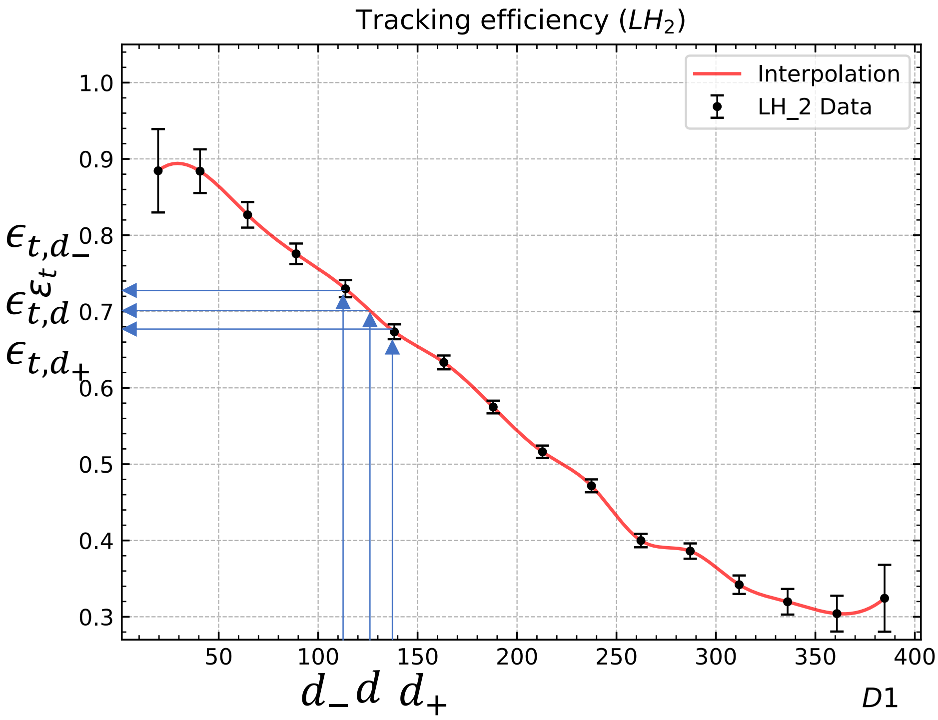

Figure 18: Global Reconstruction Efficiency curve as a function of the $D1$ occupancy variable, integrated over all kinematic bins.

For each dimuon passing event selection, the reconstruction efficiency is calculated based on its $D1$ occupancy using following equation:

$$\epsilon_i = \epsilon(D1^-) + \left(\frac{\epsilon(D1^+) - \epsilon(D1^-)}{D1^+ - D1^-}\right)\left(D1^+ - D1_i\right) \tag{8}$$

where $D1_i$ is the $D1$ occupancy for the dimuon event, and $D1^-$ and $D1^+$ are the nearest lower and upper bin edges on the global reconstruction efficiency curve. For **mixed events**, the reconstruction efficiency is calculated using an average $D1$ occupancy:

$$D1_{\text{mixed}} = \frac{D1_{\text{pos}} + D1_{\text{neg}}}{2} \tag{9}$$

An average reconstruction efficiency, $\langle \epsilon_{\mathrm{recon}} \rangle$, with correctly propagated uncertainty, is then calculated for each kinematic bin. The Global Reconstruction Efficiency curve and the 2-D plots of the average efficiency for LH2 target dimuons and LH2 mixed events are presented below.

4.1 Uncertainty Propagation

An important aspect of this procedure is the correct propagation of uncertainties. For each event in the data with a measured D1 value, an efficiency ϵ_i and its uncertainty $\delta\epsilon_i$ are determined by linear interpolation between points on the MC-derived efficiency curve. For a given event i the efficiency will be interpolated:

$$\delta\epsilon_i = \frac{1}{D1^+ - D1^-}\sqrt{\left(D1^+ - D1_i\right)^2 \delta\epsilon(D1^+)^2 + \left(D1^- - D1_i\right)^2 \delta\epsilon(D1^-)^2} \tag{10}$$

where $D1_i$ is the value of D1 for the event i, $D1^+$ is the nearest D1 value greater than $D1_i$, $D1^-$ is the nearest D1 value less than $D1_i$, $\epsilon(D1^{\pm})$ is the value of the efficiency at $D1^{\pm}$, and $\delta\epsilon(D1^{\pm})$ is the uncertainty in $\epsilon(D1^{\pm})$.

The average efficiency $\langle \epsilon \rangle$ for a bin containing N data events is the mean of the individual efficiencies:

$$\langle \epsilon \rangle = \frac{1}{N}\sum_{i=1}^{N} \epsilon_i \tag{11}$$

The uncertainty on this average, $\delta\langle \epsilon \rangle$, is based on the propagated error from the uncertainty on the MC-derived efficiency curve itself.

$$\delta_{\mathrm{prop}}\langle \epsilon \rangle = \frac{1}{N}\sqrt{\sum_{i=1}^{N} (\delta\epsilon_i)^2} \tag{12}$$

We calculate the average reconstruction efficiency and its propagated uncertainty for both target dimuons and mixed dimuons in each kinematic bin. The average reconstruction efficiency correction calculated for each kinematic bin with the propagated uncertainty for target dimuons and mixed events are shown in 2-D plots below in Figure 19.

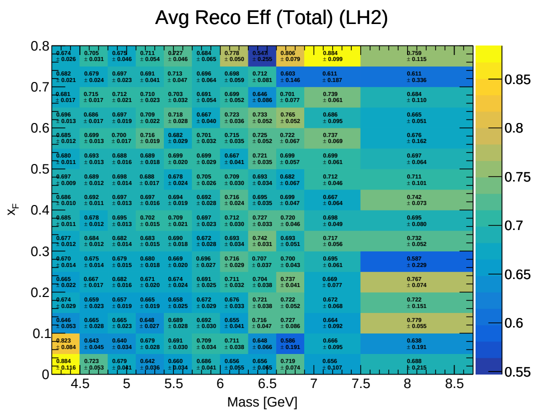

(a) LH2 average reconstruction efficiency for total

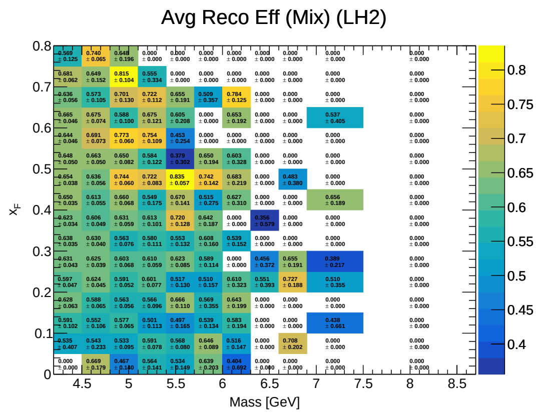

(b) LH2 average reconstruction efficiency for mix

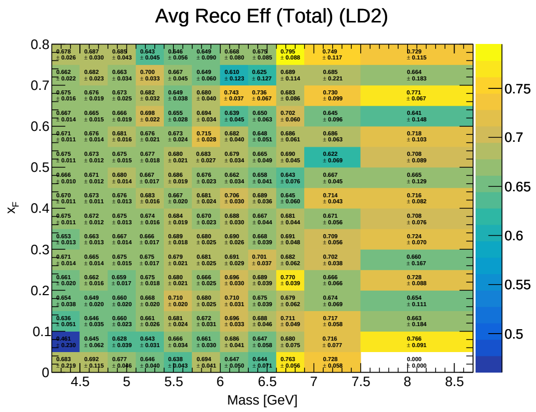

(c) LD2 average reconstruction efficiency for total

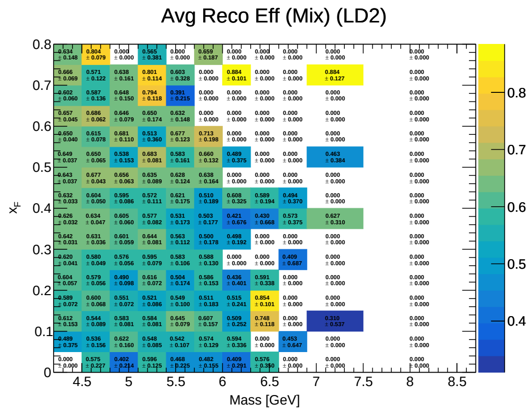

(d) LD2 average reconstruction efficiency for mix

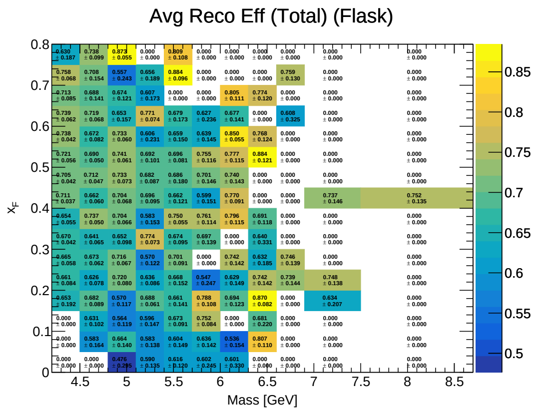

(e) Flask average reconstruction efficiency for total

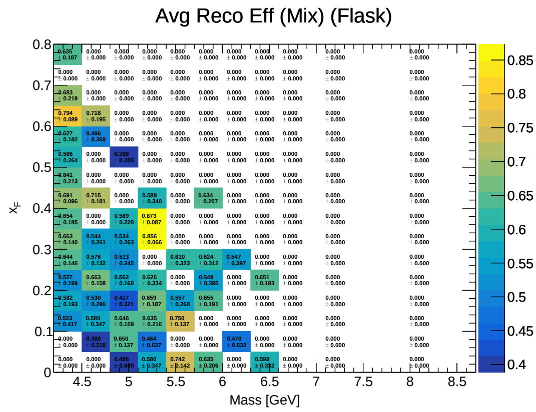

(f) Flask average reconstruction efficiency for mix

Figure 19: Average Reconstruction Efficiencies calculated each kinematic bin with the propagated uncertainties.

5 Hodoscope Efficiency Correction

Previously, a constant hodoscope efficiency correction of 0.845 ± 0.125 was used (DocDB 11383-v4). In this analysis, we calculate the hodoscope efficiency for both target dimuons and mixed dimuons on an event-by-event basis. This is done by determining the roadID for the positive track ('posRoad') and the negative track ('negRoad') and utilizing the hodoscope paddle efficiency table created by Harsha (DocDB 11467-v4).

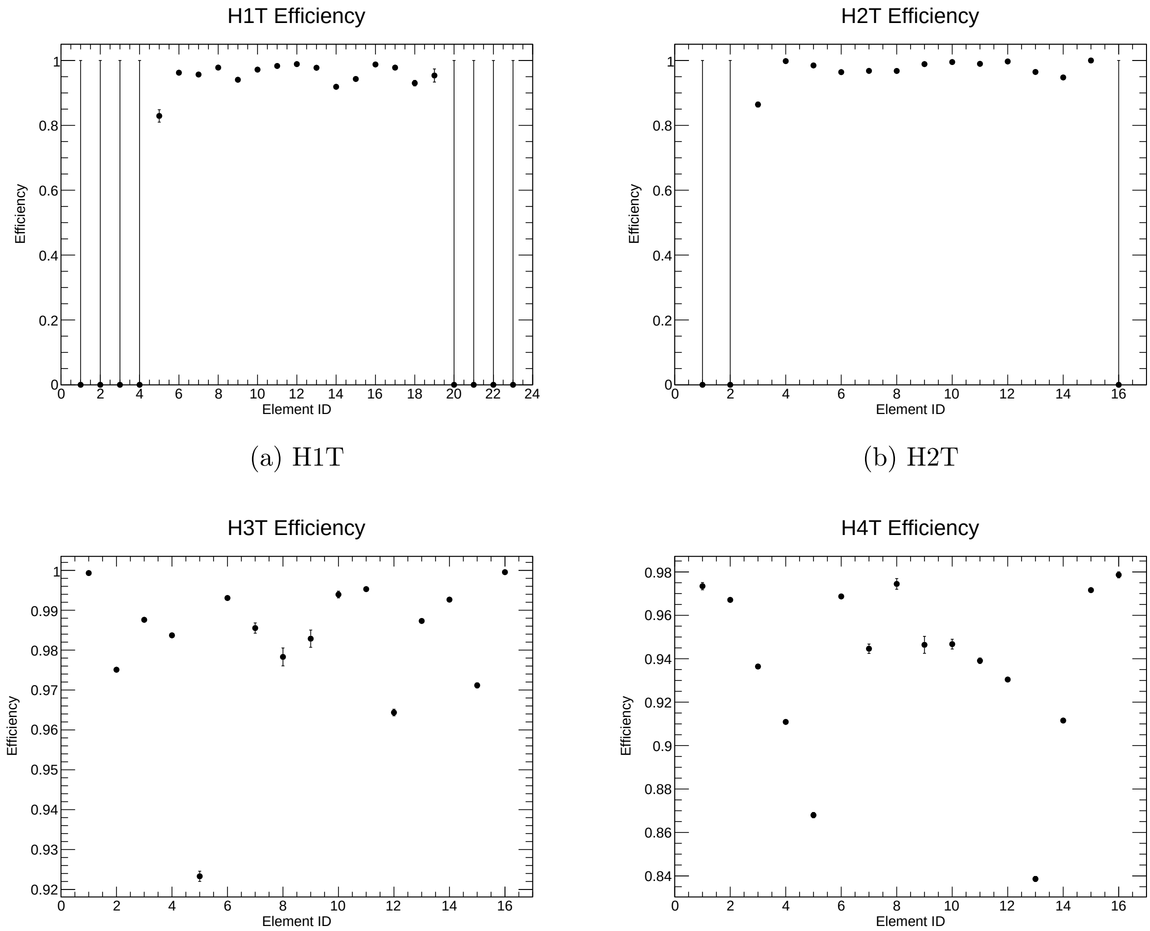

(a) H1T (b) H2T

(c) H3T (d) H4T

Figure 20: Hodoscope Paddle Efficiencies (Top Planes).

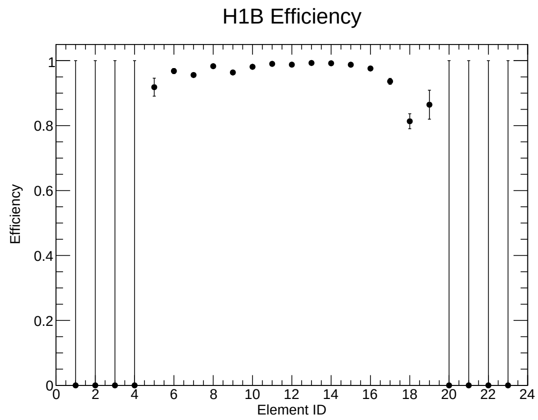

(e) H1B

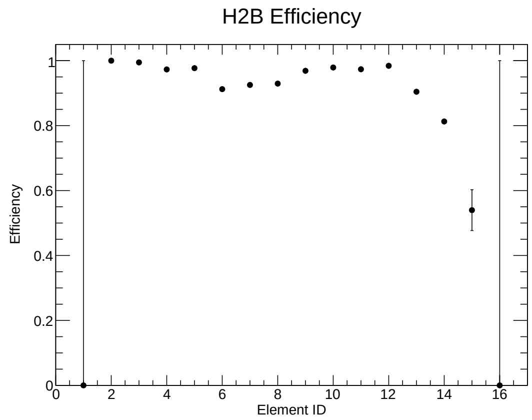

(f) H2B

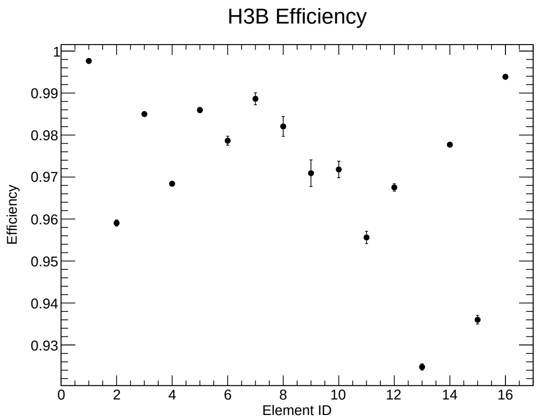

(g) H3B

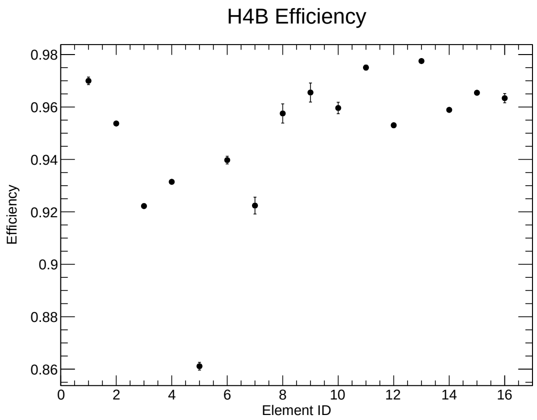

(h) H4B

Figure 20: Hodoscope Paddle Efficiencies (Bottom Planes) – Continued.

We also calculated hit distributions for each hodoscope paddle and shown below in Figure 21.

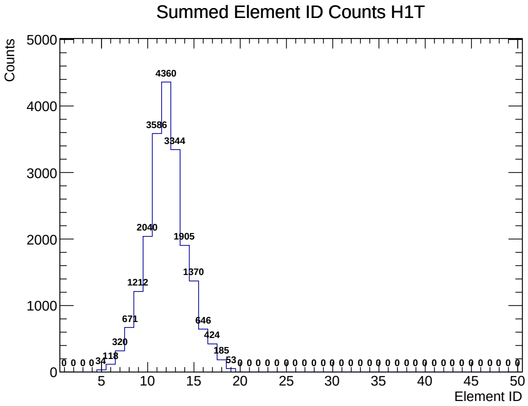

(a) H1T Plane

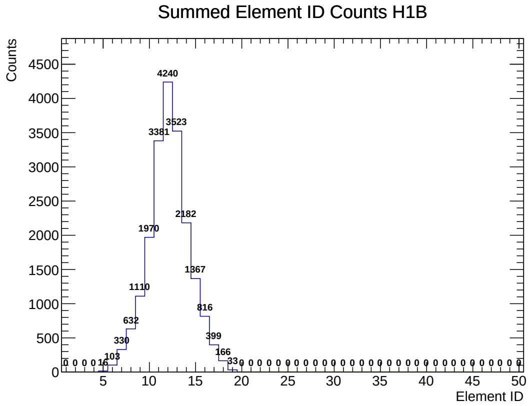

(b) H1B Plane

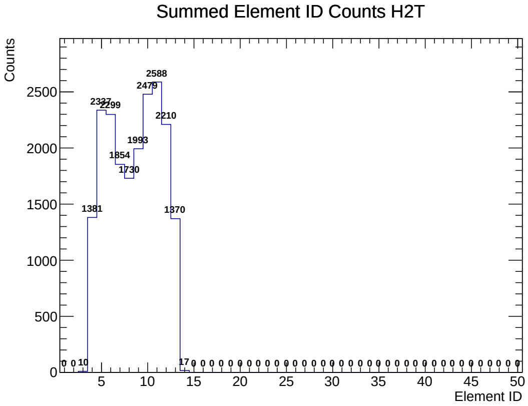

(c) H2T Plane

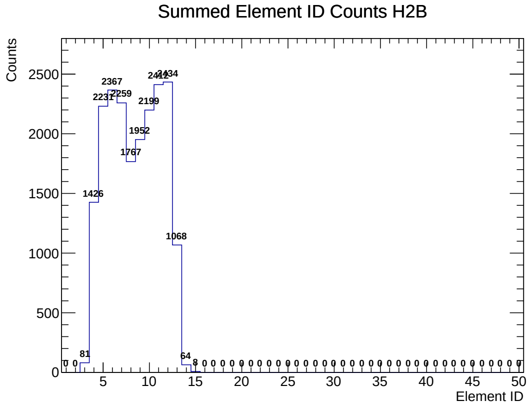

(d) H2B Plane

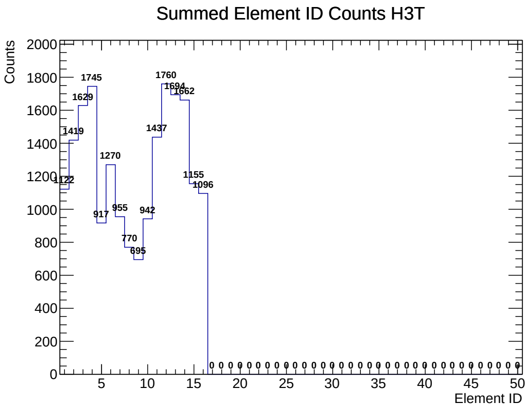

(e) H3T Plane

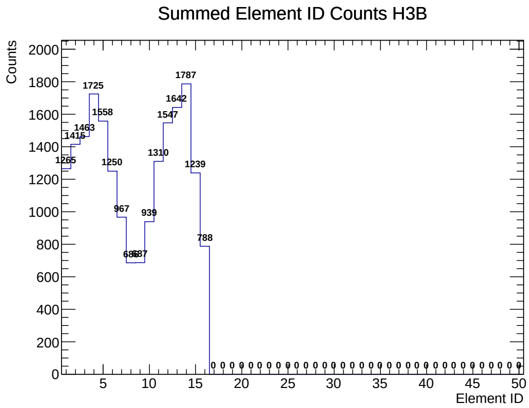

(f) H3B Plane

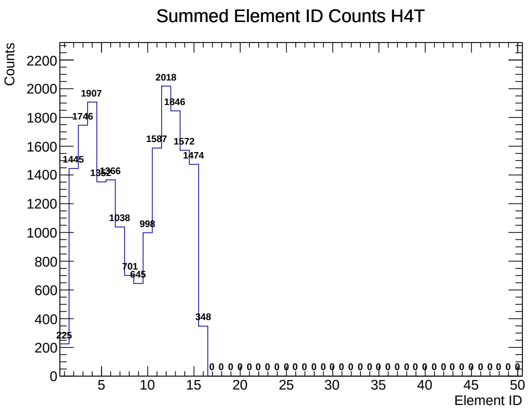

(g) H4T Plane

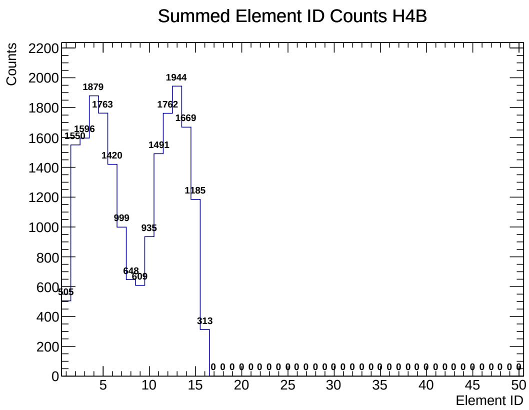

(h) H4B Plane

Figure 21: Hodoscope Paddle hit distributions arranged by Plane (Rows 1-4), Top vs Bottom.

The average hodoscope efficiency, $\langle \epsilon_{\text{hodo}} \rangle$, along with propagated uncertainty, is calculated for each kinematic bin. 2-D plots are shown below in Figure 22.

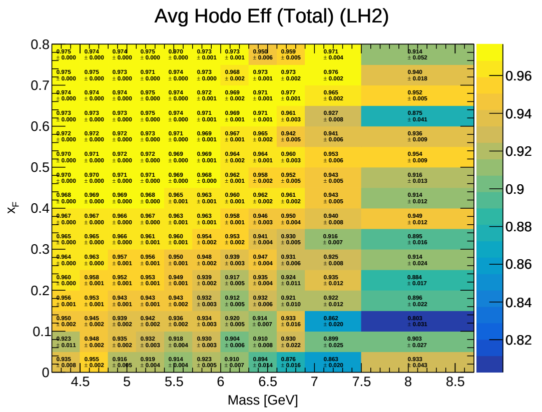

(a) LH2 average hodoscope efficiency for total

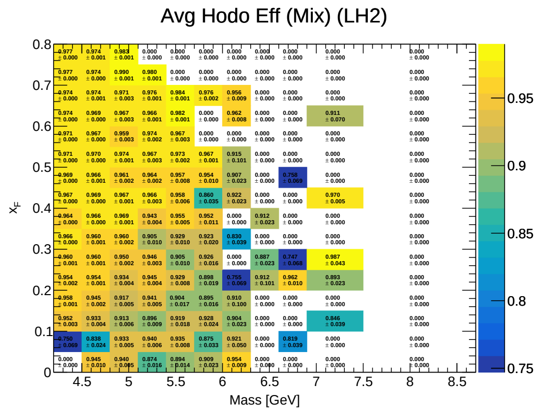

(b) LH2 average hodoscope efficiency for mix

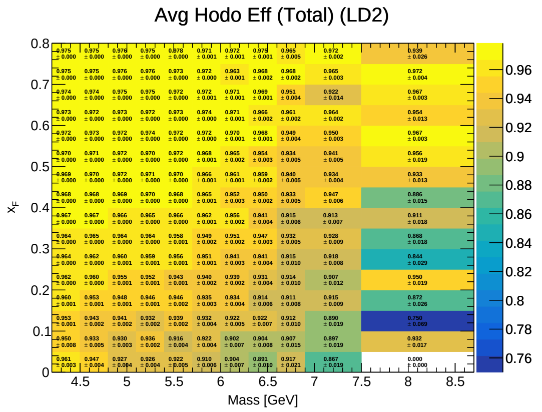

(c) LD2 average hodoscope efficiency for total

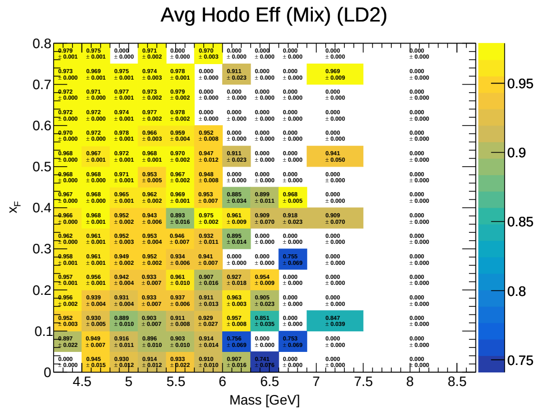

(d) LD2 average hodoscope efficiency for mix

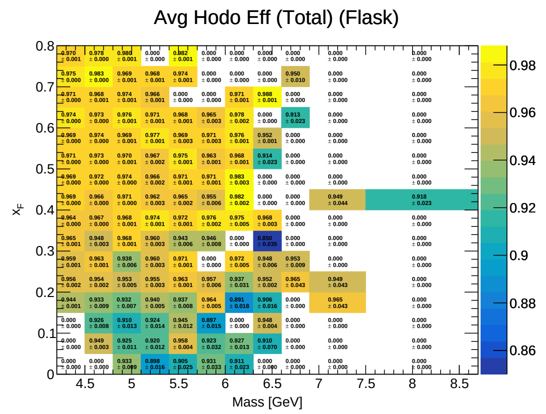

(e) Flask average hodoscope efficiency for total

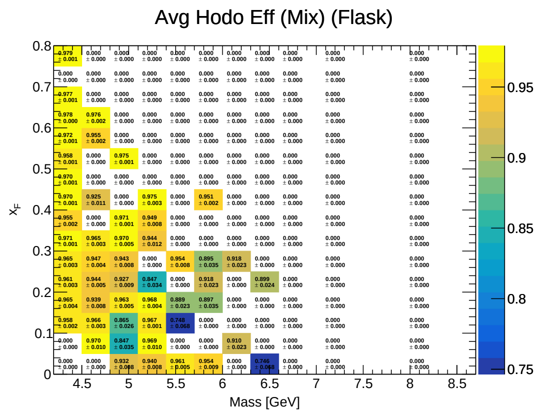

(f) Flask average hodoscope efficiency for mix

Figure 22: Average Hodoscope Efficiencies calculated each kinematic bin with the propagated uncertainties.

6 Total Efficiency Correction

The total efficiency correction $\epsilon^{i}_{\text{total}}$ for the i^{th} is calculated on a dimuon-by-dimuon basis as the product of the reconstruction and hodoscope efficiencies as defined in the equation 4.

The average total efficiencies for the total and mixed event yields, along with their propagated uncertainties, are calculated for each kinematic bin and are shown below in Figure 23.

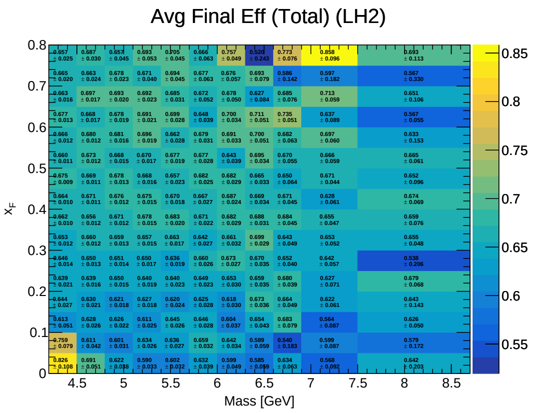

(a) LH2 average total efficiency for total

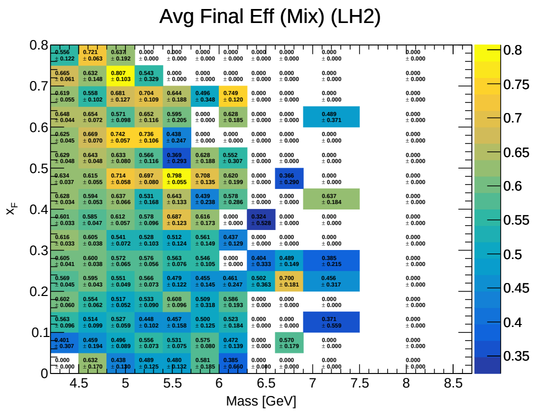

(b) LH2 average total efficiency for mix

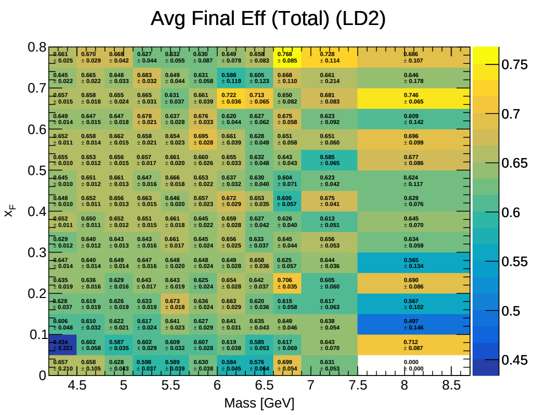

(c) LD2 average total efficiency for total

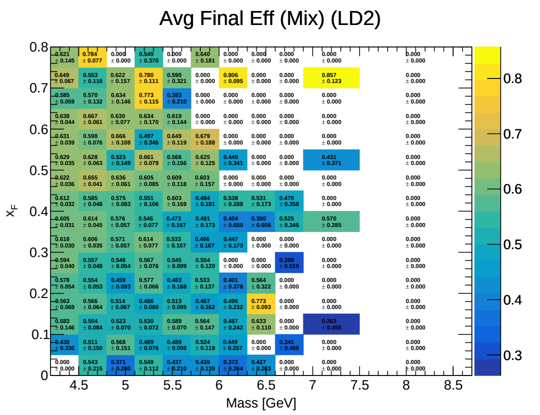

(d) LD2 average total efficiency for mix

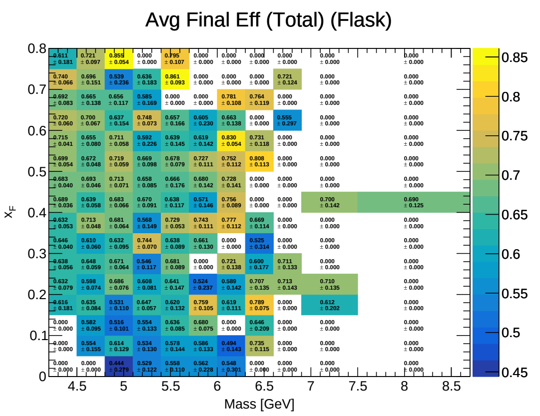

(e) Flask average total efficiency for total

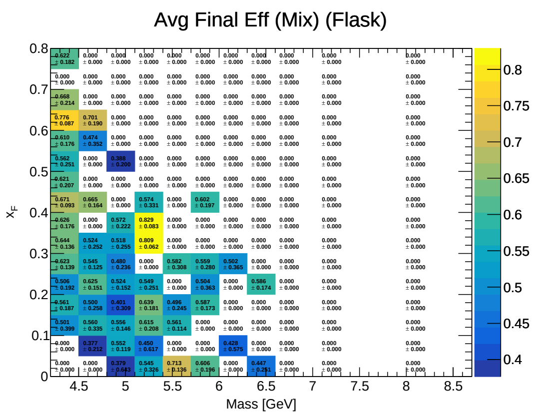

(f) Flask average total efficiency for mix

Figure 23: Average total Efficiencies calculated each kinematic bin with the propagated uncertainties.

7 Determination of Corrected Yields

With the average total efficiencies determined, we extract the corrected yields by calculating the average signal efficiency correction using the following equation:

$$\langle \epsilon_{\mathrm{sig}} \rangle = \frac{1}{Y_{\mathrm{total}} - Y_{\mathrm{mix}}} \left[\epsilon_{\mathrm{total}} Y_{\mathrm{total}} - \epsilon_{\mathrm{mix}} Y_{\mathrm{mix}} \right] \tag{13}$$

We then apply this correction factor to determine the final background-subtracted yield for the signal:

$$Y_{\mathrm{corrected}} = \frac{Y_{\mathrm{total}} - Y_{\mathrm{mix}}}{\langle \epsilon_{\mathrm{sig}} \rangle} \tag{14}$$

The resulting average signal efficiency corrections and the corrected signal yields for each target configuration are presented in Figure 24.

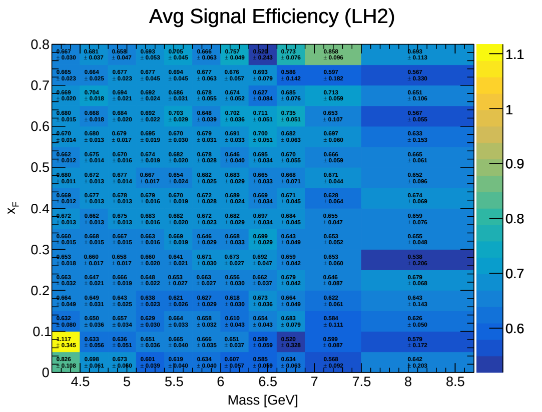

(a) LH2 average efficiency correction for signal

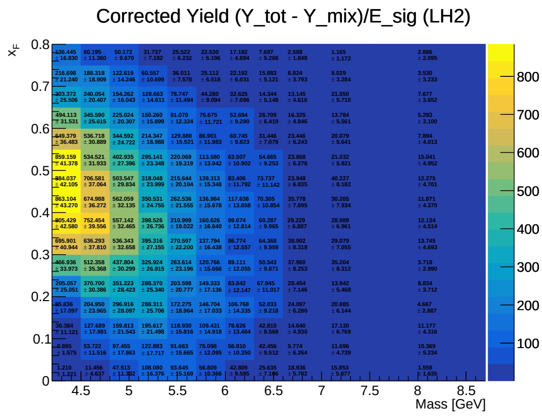

(b) Corrected yield for LH2

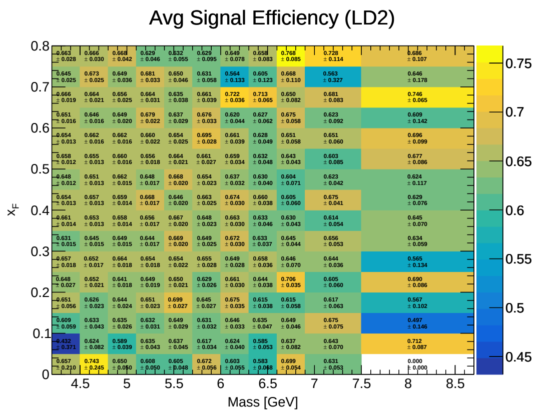

(c) LD2 average efficiency correction for signal

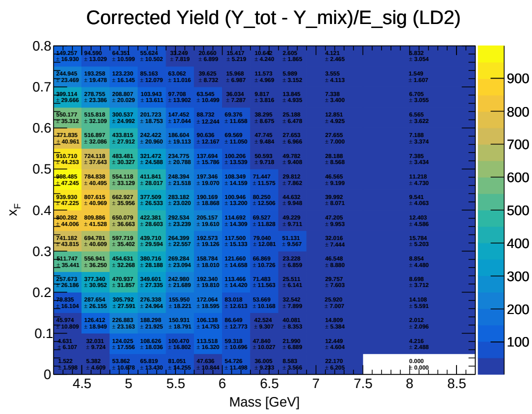

(d) Corrected yield for LD2

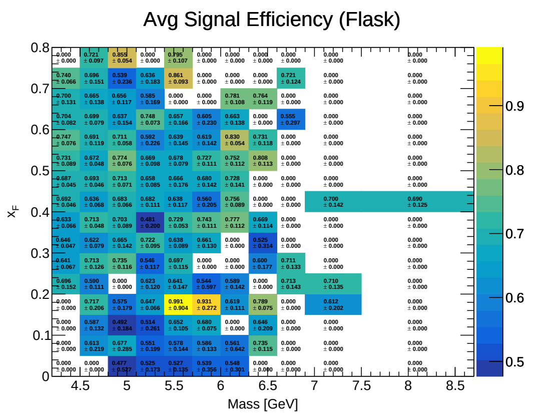

(e) Flask average efficiency correction for signal

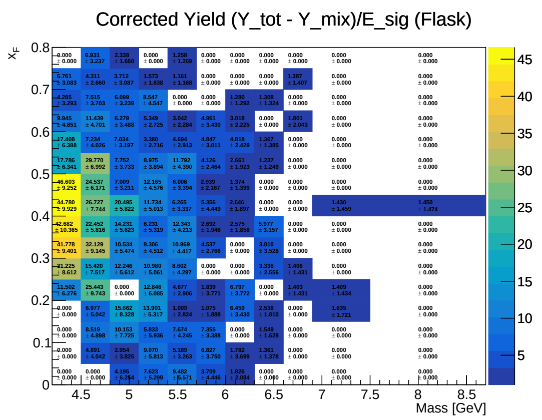

(f) Corrected yield for Flask

Figure 24: Average efficiency correction for signal and final corrected yields.

8 Appendix: Event Selection Criteria (Chuck Cuts)

The event selection criteria, commonly referred to as "Chuck Cuts," are designed to select high-quality dimuon events originating from the target while rejecting backgrounds from the beam dump, upstream interactions, and cosmic rays. The cuts are applied at three levels: single track quality, dimuon vertex/kinematics, and detector occupancy.

In the following tables, the beam vertical offset is denoted as $y_{\mathrm{beam}} = 1.6$ cm.

8.1 Single Track Cuts

These cuts are applied individually to both the positive and negative muon tracks to ensure they are well-reconstructed and pass through the spectrometer magnet apertures correctly.

Table 1: Single track selection criteria.

Variable	**Condition**
Track Fit Quality	
Target χ^2	$\chi^2_{\mathrm{target}} < 15$
Reduced χ^2	$\chi^2/(N_{\mathrm{hits}} - 5) < 12$
Vertex Assumption	$\chi^2_{\mathrm{target}} < 1.5 \times \chi^2_{\mathrm{dump}}$ AND $\chi^2_{\mathrm{target}} < 1.5 \times \chi^2_{\mathrm{upstream}}$
Hits & Geometry	
Number of Hits	$N_{\mathrm{hits}} > 13$
Station 1 Z-Momentum	$9 < p_{z,\mathrm{st1}} < 75$ GeV/c
Single Track Vertex z	$-320 < z_v < -5$ cm
Aperture & Trajectory	
Radial pos. at target ($z \approx -130$ cm)	$x^2 + (y - y_{\mathrm{beam}})^2 < 320$ cm^2
Radial pos. at dump ($z \approx 50$ cm)	$16 < x^2 + (y - y_{\mathrm{beam}})^2 < 1100$ cm^2
Vertical Focusing	$y_{\mathrm{st1}}/y_{\mathrm{st3}} < 1$
Vertical Projection	$y_{\mathrm{st1}} \cdot y_{\mathrm{st3}} > 0$
Min Vertical Momentum	$\lvert p_{y,\mathrm{st1}}\rvert > 0.02$ GeV/c
Momentum Conservation	
KMag Momentum Kick	$\lvert\lvert p_{x,\mathrm{st1}} - p_{x,\mathrm{st3}}\rvert - 0.416\rvert < 0.008$ GeV/c
Vertical Bend (Null)	$\lvert p_{y,\mathrm{st1}} - p_{y,\mathrm{st3}}\rvert < 0.008$ GeV/c
Longitudinal (Null)	$\lvert p_{z,\mathrm{st1}} - p_{z,\mathrm{st3}}\rvert < 0.08$ GeV/c

8.2 Dimuon Cuts

After forming a dimuon pair, the following cuts ensure the vertex is valid and the kinematics fall within the trustworthy region of the spectrometer acceptance.

8.3 Occupancy and Topology Cuts

These cuts remove events with high detector activity (which complicates reconstruction) and ensure the two muons pass through opposite sides of the spectrometer (the standard "top/bottom" trigger topology).

Table 2: Dimuon kinematic and vertex selection criteria.

Variable	Condition
Vertex Position	
Transverse Offset (x)	$\lvert dx \rvert < 0.25$ cm
Vertical Offset (y)	$\lvert dy - y_{\text{beam}} \rvert < 0.22$ cm
Radial Vertex	$dx^2 + (dy - y_{\text{beam}})^2 < 0.06$ cm^2
Longitudinal Vertex (z)	$-280 < dz < -5$ cm
Vertex Fit Quality	$\chi^2_{\text{dimuon}} < 18$
Vertex Consistency	$\lvert \chi^2_{\text{trk1}} + \chi^2_{\text{trk2}} - \chi^2_{\text{dimuon}} \rvert < 2$
Kinematics	
Invariant Mass	$4.2 < M_{\mu\mu} < 8.8$ GeV/c^2
Feynman-x	$-0.1 < x_F < 0.95$
Transverse Scaling x_T	$0.05 < x_T \leq 0.58$
Costh (Collins-Soper)	$\lvert \cos\theta \rvert < 0.5$
Longitudinal Momentum	$38 < p_z < 116$ GeV/c
Transverse Momentum limits	$\lvert dp_x \rvert < 1.8$ GeV/c, $\lvert dp_y \rvert < 2.0$ GeV/c
Total p_T	$dp_x^2 + dp_y^2 < 5.0$ (GeV/c)^2
Track Separation	sep < 270 cm

Table 3: Occupancy and topological cuts.

Variable	Condition
Chamber Occupancy	
Drift Chamber 1 Hits	$D1 < 400$
Drift Chamber 2 Hits	$D2 < 400$
Drift Chamber 3 Hits	$D3 < 400$
Total Chamber Hits	$D1 + D2 + D3 < 1000$
Topology	
Opposite Quadrants	$y^{\text{trk1}}_{\text{st3}} \cdot y^{\text{trk2}}_{\text{st3}} < 0$
Total Hits on Tracks	$N^{\text{trk1}}_{\text{hits}} + N^{\text{trk2}}_{\text{hits}} > 29$
Station 1 Hits Sum	$N^{\text{trk1}}_{\text{hits, st1}} + N^{\text{trk2}}_{\text{hits, st1}} > 8$
Station 1 X-Sum	$\lvert x^{\text{trk1}}_{\text{st1}} + x^{\text{trk2}}_{\text{st1}} \rvert < 42$ cm

9 Appendix: Efficiency Plots

This appendix contains the efficiency studies used in this analysis. Figures 19, 22, and 21 show the relevant efficiency and distribution maps.

10 Appendix: Table of Systematic Errors

Table 4: Detailed Systematic Error calculation for Bins in x_F and Mass

x_F Bin	Mass Bin (GeV)	Trigger Eff.	Acceptance	k-Tracker Eff.	Total Syst.
[0.00 - 0.05)	[4.50 - 4.80)	0.779025	1.873238	0.946767	2.238809
[0.00 - 0.05)	[4.80 - 5.10)	0.058272	0.052304	0.009351	0.078860
[0.00 - 0.05)	[5.10 - 5.40)	0.081048	0.047749	0.018181	0.095809
[0.00 - 0.05)	[5.40 - 5.70)	0.033849	0.013951	0.004059	0.036835
[0.00 - 0.05)	[5.70 - 6.00)	0.025896	0.009169	0.005236	0.027966
[0.00 - 0.05)	[6.00 - 6.30)	0.019771	0.006552	0.003990	0.021207
[0.00 - 0.05)	[6.30 - 6.60)	0.019741	0.006295	0.007003	0.021872
[0.00 - 0.05)	[6.60 - 6.90)	0.012449	0.004049	0.002978	0.013425
[0.00 - 0.05)	[6.90 - 7.50)	0.007375	0.001898	0.002170	0.007919
[0.00 - 0.05)	[7.50 - 8.70)	0.000946	0.000252	0.000628	0.001163
[0.05 - 0.10)	[4.50 - 4.80)	0.284881	0.378813	0.155516	0.498841
[0.05 - 0.10)	[4.80 - 5.10)	0.166470	0.128867	0.041569	0.214586
[0.05 - 0.10)	[5.10 - 5.40)	0.055664	0.025882	0.005169	0.061605
[0.05 - 0.10)	[5.40 - 5.70)	0.032285	0.011302	0.003966	0.034436
[0.05 - 0.10)	[5.70 - 6.00)	0.019937	0.006339	0.002229	0.021039
[0.05 - 0.10)	[6.00 - 6.30)	0.018107	0.005156	0.001957	0.018928
[0.05 - 0.10)	[6.30 - 6.60)	0.015415	0.004246	0.003557	0.016380
[0.05 - 0.10)	[6.60 - 6.90)	0.002562	0.000686	0.001166	0.002897
[0.05 - 0.10)	[6.90 - 7.50)	0.004064	0.000910	0.001134	0.004316
[0.05 - 0.10)	[7.50 - 8.70)	0.003523	0.000764	0.001074	0.003762
[0.10 - 0.15)	[4.50 - 4.80)	0.198459	0.182806	0.040656	0.272868
[0.10 - 0.15)	[4.80 - 5.10)	0.083380	0.040798	0.013031	0.093736
[0.10 - 0.15)	[5.10 - 5.40)	0.081948	0.031238	0.010558	0.088333
[0.10 - 0.15)	[5.40 - 5.70)	0.030329	0.009540	0.002815	0.031918
[0.10 - 0.15)	[5.70 - 6.00)	0.024458	0.006894	0.002083	0.025497
[0.10 - 0.15)	[6.00 - 6.30)	0.023572	0.006173	0.002268	0.024472
[0.10 - 0.15)	[6.30 - 6.60)	0.011184	0.002813	0.001083	0.011583
[0.10 - 0.15)	[6.60 - 6.90)	0.006021	0.001560	0.001047	0.006307
[0.10 - 0.15)	[6.90 - 7.50)	0.004337	0.000867	0.000718	0.004481
[0.10 - 0.15)	[7.50 - 8.70)	0.002871	0.000555	0.000388	0.002950
[0.15 - 0.20)	[4.50 - 4.80)	0.124062	0.075232	0.015770	0.145945
[0.15 - 0.20)	[4.80 - 5.10)	0.115363	0.046469	0.012767	0.125024
[0.15 - 0.20)	[5.10 - 5.40)	0.072817	0.024387	0.004930	0.076950
[0.15 - 0.20)	[5.40 - 5.70)	0.041137	0.011396	0.003480	0.042828
[0.15 - 0.20)	[5.70 - 6.00)	0.035444	0.009302	0.002872	0.036756
[0.15 - 0.20)	[6.00 - 6.30)	0.020001	0.004856	0.001682	0.020651
[0.15 - 0.20)	[6.30 - 6.60)	0.010531	0.002410	0.000921	0.010843
[0.15 - 0.20)	[6.60 - 6.90)	0.008260	0.001887	0.001449	0.008596
[0.15 - 0.20)	[6.90 - 7.50)	0.002937	0.000541	0.000443	0.003019
[0.15 - 0.20)	[7.50 - 8.70)	0.000973	0.000170	0.000400	0.001065
[0.20 - 0.25)	[4.20 - 4.50)	0.166120	0.120909	0.026450	0.207158
[0.20 - 0.25)	[4.50 - 4.80)	0.145103	0.071032	0.012123	0.162010
[0.20 - 0.25)	[4.80 - 5.10)	0.102147	0.034999	0.005624	0.108123
[0.20 - 0.25)	[5.10 - 5.40)	0.053289	0.015003	0.002962	0.055440
[0.20 - 0.25)	[5.40 - 5.70)	0.041865	0.010845	0.002727	0.043332

Cont'd on next page

Table 4: (Continued)

x_F Bin	Mass Bin (GeV)	Trigger Eff.	Acceptance	k-Tracker Eff.	Total Syst.
[0.20 - 0.25)	[5.70 - 6.00)	0.027889	0.006527	0.001469	0.028680
[0.20 - 0.25)	[6.00 - 6.30)	0.013039	0.002957	0.001025	0.013410
[0.20 - 0.25)	[6.30 - 6.60)	0.016485	0.003541	0.001461	0.016924
[0.20 - 0.25)	[6.60 - 6.90)	0.006353	0.001394	0.000605	0.006533
[0.20 - 0.25)	[6.90 - 7.50)	0.001365	0.000229	0.000204	0.001398
[0.20 - 0.25)	[7.50 - 8.70)	0.001336	0.000211	0.000136	0.001359
[0.25 - 0.30)	[4.20 - 4.50)	0.141343	0.072939	0.010257	0.159384
[0.25 - 0.30)	[4.50 - 4.80)	0.130167	0.051529	0.006463	0.140145
[0.25 - 0.30)	[4.80 - 5.10)	0.079605	0.023998	0.003471	0.083216
[0.25 - 0.30)	[5.10 - 5.40)	0.054612	0.014272	0.002683	0.056510
[0.25 - 0.30)	[5.40 - 5.70)	0.038571	0.009218	0.001867	0.039701
[0.25 - 0.30)	[5.70 - 6.00)	0.023376	0.005079	0.001591	0.023974
[0.25 - 0.30)	[6.00 - 6.30)	0.017654	0.003770	0.001225	0.018093
[0.25 - 0.30)	[6.30 - 6.60)	0.007693	0.001519	0.000560	0.007862
[0.25 - 0.30)	[6.60 - 6.90)	0.007726	0.001536	0.001007	0.007941
[0.25 - 0.30)	[6.90 - 7.50)	0.005124	0.000778	0.000489	0.005206
[0.25 - 0.30)	[7.50 - 8.70)	0.000519	0.000076	0.000209	0.000565
[0.30 - 0.35)	[4.20 - 4.50)	0.143223	0.062852	0.006469	0.156541
[0.30 - 0.35)	[4.50 - 4.80)	0.100283	0.033699	0.003193	0.105842
[0.30 - 0.35)	[4.80 - 5.10)	0.078522	0.020901	0.002863	0.081307
[0.30 - 0.35)	[5.10 - 5.40)	0.052272	0.012726	0.001692	0.053826
[0.30 - 0.35)	[5.40 - 5.70)	0.035353	0.007742	0.001569	0.036225
[0.30 - 0.35)	[5.70 - 6.00)	0.019840	0.004222	0.001174	0.020318
[0.30 - 0.35)	[6.00 - 6.30)	0.016108	0.003287	0.001254	0.016488
[0.30 - 0.35)	[6.30 - 6.60)	0.010060	0.002023	0.000634	0.010281
[0.30 - 0.35)	[6.60 - 6.90)	0.008018	0.001569	0.000793	0.008208
[0.30 - 0.35)	[6.90 - 7.50)	0.003694	0.000533	0.000421	0.003756
[0.30 - 0.35)	[7.50 - 8.70)	0.001747	0.000242	0.000186	0.001773
[0.35 - 0.40)	[4.20 - 4.50)	0.106457	0.037922	0.003043	0.113051
[0.35 - 0.40)	[4.50 - 4.80)	0.100531	0.029480	0.003146	0.104811
[0.35 - 0.40)	[4.80 - 5.10)	0.072502	0.018895	0.002326	0.074960
[0.35 - 0.40)	[5.10 - 5.40)	0.048131	0.010864	0.001538	0.049365
[0.35 - 0.40)	[5.40 - 5.70)	0.020800	0.004392	0.000837	0.021275
[0.35 - 0.40)	[5.70 - 6.00)	0.020491	0.004143	0.000980	0.020928
[0.35 - 0.40)	[6.00 - 6.30)	0.013363	0.002624	0.000720	0.013637
[0.35 - 0.40)	[6.30 - 6.60)	0.006047	0.001135	0.000396	0.006165
[0.35 - 0.40)	[6.60 - 6.90)	0.005933	0.001107	0.000667	0.006072
[0.35 - 0.40)	[6.90 - 7.50)	0.003348	0.000459	0.000269	0.003390
[0.35 - 0.40)	[7.50 - 8.70)	0.001436	0.000183	0.000247	0.001469
[0.40 - 0.45)	[4.20 - 4.50)	0.099323	0.033040	0.002941	0.104716
[0.40 - 0.45)	[4.50 - 4.80)	0.075954	0.020641	0.002128	0.078738
[0.40 - 0.45)	[4.80 - 5.10)	0.055286	0.012835	0.001577	0.056778
[0.40 - 0.45)	[5.10 - 5.40)	0.038052	0.008469	0.001399	0.039008
[0.40 - 0.45)	[5.40 - 5.70)	0.028172	0.005715	0.000987	0.028763
[0.40 - 0.45)	[5.70 - 6.00)	0.015105	0.002920	0.000688	0.015400
[0.40 - 0.45)	[6.00 - 6.30)	0.014939	0.002774	0.000734	0.015213
[0.40 - 0.45)	[6.30 - 6.60)	0.012131	0.002291	0.000940	0.012381
[0.40 - 0.45)	[6.60 - 6.90)	0.005773	0.001030	0.000398	0.005877

Cont'd on next page

Table 4: (Continued)

x_F Bin	Mass Bin (GeV)	Trigger Eff.	Acceptance	k-Tracker Eff.	Total Syst.
[0.40 - 0.45)	[6.90 - 7.50)	0.002557	0.000353	0.000241	0.002593
[0.40 - 0.45)	[7.50 - 8.70)	0.000491	0.000061	0.000040	0.000496
[0.45 - 0.50)	[4.20 - 4.50)	0.078635	0.023049	0.002059	0.081969
[0.45 - 0.50)	[4.50 - 4.80)	0.067541	0.017403	0.001706	0.069768
[0.45 - 0.50)	[4.80 - 5.10)	0.053760	0.012443	0.001688	0.055207
[0.45 - 0.50)	[5.10 - 5.40)	0.028610	0.005965	0.001078	0.029245
[0.45 - 0.50)	[5.40 - 5.70)	0.020809	0.004172	0.000821	0.021239
[0.45 - 0.50)	[5.70 - 6.00)	0.015482	0.002928	0.000738	0.015774
[0.45 - 0.50)	[6.00 - 6.30)	0.010741	0.001999	0.000674	0.010946
[0.45 - 0.50)	[6.30 - 6.60)	0.011477	0.002063	0.000873	0.011694
[0.45 - 0.50)	[6.60 - 6.90)	0.004200	0.000754	0.000554	0.004303
[0.45 - 0.50)	[6.90 - 7.50)	0.004274	0.000573	0.000231	0.004319
[0.45 - 0.50)	[7.50 - 8.70)	0.000999	0.000121	0.000098	0.001011
[0.50 - 0.55)	[4.20 - 4.50)	0.091374	0.025832	0.003131	0.095007
[0.50 - 0.55)	[4.50 - 4.80)	0.038797	0.009116	0.001196	0.039872
[0.50 - 0.55)	[4.80 - 5.10)	0.035794	0.007792	0.001215	0.036652
[0.50 - 0.55)	[5.10 - 5.40)	0.025971	0.005366	0.000845	0.026533
[0.50 - 0.55)	[5.40 - 5.70)	0.017990	0.003538	0.000653	0.018346
[0.50 - 0.55)	[5.70 - 6.00)	0.010504	0.001914	0.000561	0.010691
[0.50 - 0.55)	[6.00 - 6.30)	0.006640	0.001204	0.000587	0.006773
[0.50 - 0.55)	[6.30 - 6.60)	0.007154	0.001324	0.000432	0.007288
[0.50 - 0.55)	[6.60 - 6.90)	0.004000	0.000731	0.000474	0.004094
[0.50 - 0.55)	[6.90 - 7.50)	0.001946	0.000254	0.000172	0.001970
[0.50 - 0.55)	[7.50 - 8.70)	0.001279	0.000149	0.000130	0.001294
[0.55 - 0.60)	[4.20 - 4.50)	0.049012	0.013093	0.001356	0.050748
[0.55 - 0.60)	[4.50 - 4.80)	0.045199	0.010565	0.001338	0.046436
[0.55 - 0.60)	[4.80 - 5.10)	0.031162	0.006899	0.001131	0.031937
[0.55 - 0.60)	[5.10 - 5.40)	0.019065	0.003784	0.000735	0.019451
[0.55 - 0.60)	[5.40 - 5.70)	0.011066	0.002143	0.000544	0.011285
[0.55 - 0.60)	[5.70 - 6.00)	0.007673	0.001386	0.000453	0.007810
[0.55 - 0.60)	[6.00 - 6.30)	0.003981	0.000698	0.000228	0.004048
[0.55 - 0.60)	[6.30 - 6.60)	0.003434	0.000599	0.000281	0.003497
[0.55 - 0.60)	[6.60 - 6.90)	0.003400	0.000586	0.000348	0.003468
[0.55 - 0.60)	[6.90 - 7.50)	0.002152	0.000282	0.000214	0.002181
[0.55 - 0.60)	[7.50 - 8.70)	0.000563	0.000065	0.000074	0.000571
[0.60 - 0.65)	[4.20 - 4.50)	0.040173	0.010809	0.001161	0.041617
[0.60 - 0.65)	[4.50 - 4.80)	0.024563	0.005615	0.000889	0.025212
[0.60 - 0.65)	[4.80 - 5.10)	0.017374	0.003688	0.000696	0.017775
[0.60 - 0.65)	[5.10 - 5.40)	0.011024	0.002225	0.000393	0.011254
[0.60 - 0.65)	[5.40 - 5.70)	0.007261	0.001362	0.000352	0.007396
[0.60 - 0.65)	[5.70 - 6.00)	0.006245	0.001139	0.000455	0.006364
[0.60 - 0.65)	[6.00 - 6.30)	0.004809	0.000872	0.000317	0.004898
[0.60 - 0.65)	[6.30 - 6.60)	0.003639	0.000641	0.000299	0.003707
[0.60 - 0.65)	[6.60 - 6.90)	0.001526	0.000273	0.000098	0.001554
[0.60 - 0.65)	[6.90 - 7.50)	0.001164	0.000147	0.000132	0.001181
[0.60 - 0.65)	[7.50 - 8.70)	0.000334	0.000038	0.000062	0.000342
[0.65 - 0.70)	[4.20 - 4.50)	0.024537	0.006446	0.000859	0.025384
[0.65 - 0.70)	[4.50 - 4.80)	0.018367	0.004297	0.000734	0.018877

Cont'd on next page

Table 4: (Continued)

x_F Bin	Mass Bin (GeV)	Trigger Eff.	Acceptance	k-Tracker Eff.	Total Syst.
[0.65 - 0.70)	[4.80 - 5.10)	0.010196	0.002166	0.000407	0.010432
[0.65 - 0.70)	[5.10 - 5.40)	0.008613	0.001753	0.000384	0.008798
[0.65 - 0.70)	[5.40 - 5.70)	0.008247	0.001614	0.000508	0.008419
[0.65 - 0.70)	[5.70 - 6.00)	0.004495	0.000836	0.000349	0.004586
[0.65 - 0.70)	[6.00 - 6.30)	0.002948	0.000528	0.000258	0.003006
[0.65 - 0.70)	[6.30 - 6.60)	0.000881	0.000156	0.000132	0.000905
[0.65 - 0.70)	[6.60 - 6.90)	0.001730	0.000297	0.000210	0.001768
[0.65 - 0.70)	[6.90 - 7.50)	0.002013	0.000264	0.000280	0.002049
[0.65 - 0.70)	[7.50 - 8.70)	0.004838	0.000546	0.017062	0.017743
[0.70 - 0.75)	[4.20 - 4.50)	0.018003	0.004826	0.000928	0.018662
[0.70 - 0.75)	[4.50 - 4.80)	0.014316	0.003395	0.000682	0.014729
[0.70 - 0.75)	[4.80 - 5.10)	0.009071	0.001949	0.000519	0.009293
[0.70 - 0.75)	[5.10 - 5.40)	0.005102	0.001052	0.000465	0.005230
[0.70 - 0.75)	[5.40 - 5.70)	0.002947	0.000565	0.000295	0.003015
[0.70 - 0.75)	[5.70 - 6.00)	0.002329	0.000432	0.000339	0.002393
[0.70 - 0.75)	[6.00 - 6.30)	0.002535	0.000456	0.000594	0.002644
[0.70 - 0.75)	[6.30 - 6.60)	0.001917	0.000343	0.000707	0.002072
[0.75 - 0.80)	[4.20 - 4.50)	0.012861	0.003466	0.001181	0.013372
[0.75 - 0.80)	[4.50 - 4.80)	0.002016	0.000478	0.000132	0.002076
[0.75 - 0.80)	[4.80 - 5.10)	0.019900	0.004388	0.022716	0.030517

11 Appendix: Table of Cross-Section Values

Table 5: Detailed cross-section calculation for Bins in x_F and Mass

x_F Bin	Mass Bin (GeV)	Bin Center (GeV)	Bin Average (GeV)	Cross-Section (nb-GeV^2)	stat. error (nb-GeV^2)	syst. error (nb-GeV^2)
[0.00, 0.05)	[4.5, 4.8)	4.650	4.740	5.266×10^{0}	3.059×10^{0}	2.239×10^{0}
[0.00, 0.05)	[4.8, 5.1)	4.950	5.006	3.939×10^{-1}	2.024×10^{-1}	7.886×10^{-2}
[0.00, 0.05)	[5.1, 5.4)	5.250	5.250	5.479×10^{-1}	1.864×10^{-1}	9.581×10^{-2}
[0.00, 0.05)	[5.4, 5.7)	5.550	5.512	2.288×10^{-1}	9.988×10^{-2}	3.684×10^{-2}
[0.00, 0.05)	[5.7, 6.0)	5.850	5.828	1.751×10^{-1}	7.393×10^{-2}	2.797×10^{-2}
[0.00, 0.05)	[6.0, 6.3)	6.150	6.178	1.336×10^{-1}	4.716×10^{-2}	2.121×10^{-2}
[0.00, 0.05)	[6.3, 6.6)	6.450	6.432	1.334×10^{-1}	4.608×10^{-2}	2.187×10^{-2}
[0.00, 0.05)	[6.6, 6.9)	6.750	6.749	8.415×10^{-2}	2.777×10^{-2}	1.343×10^{-2}
[0.00, 0.05)	[6.9, 7.5)	7.200	7.171	4.985×10^{-2}	1.846×10^{-2}	7.919×10^{-3}
[0.00, 0.05)	[7.5, 8.7)	8.100	7.914	6.397×10^{-3}	6.502×10^{-3}	1.163×10^{-3}
[0.05, 0.10)	[4.5, 4.8)	4.650	4.627	1.926×10^{0}	1.237×10^{0}	4.988×10^{-1}
[0.05, 0.10)	[4.8, 5.1)	4.950	4.944	1.125×10^{0}	3.799×10^{-1}	2.146×10^{-1}
[0.05, 0.10)	[5.1, 5.4)	5.250	5.251	3.763×10^{-1}	1.199×10^{-1}	6.160×10^{-2}
[0.05, 0.10)	[5.4, 5.7)	5.550	5.526	2.182×10^{-1}	6.716×10^{-2}	3.444×10^{-2}
[0.05, 0.10)	[5.7, 6.0)	5.850	5.865	1.348×10^{-1}	5.227×10^{-2}	2.104×10^{-2}
[0.05, 0.10)	[6.0, 6.3)	6.150	6.086	1.224×10^{-1}	4.329×10^{-2}	1.893×10^{-2}
[0.05, 0.10)	[6.3, 6.6)	6.450	6.408	1.042×10^{-1}	3.840×10^{-2}	1.638×10^{-2}
[0.05, 0.10)	[6.6, 6.9)	6.750	6.725	1.732×10^{-2}	1.601×10^{-2}	2.897×10^{-3}
[0.05, 0.10)	[6.9, 7.5)	7.200	7.125	2.747×10^{-2}	1.126×10^{-2}	4.316×10^{-3}
[0.05, 0.10)	[7.5, 8.7)	8.100	7.731	2.382×10^{-2}	1.045×10^{-2}	3.762×10^{-3}
[0.10, 0.15)	[4.5, 4.8)	4.650	4.685	1.342×10^{0}	4.340×10^{-1}	2.729×10^{-1}
[0.10, 0.15)	[4.8, 5.1)	4.950	4.956	5.636×10^{-1}	1.621×10^{-1}	9.374×10^{-2}
[0.10, 0.15)	[5.1, 5.4)	5.250	5.231	5.540×10^{-1}	1.229×10^{-1}	8.833×10^{-2}
[0.10, 0.15)	[5.4, 5.7)	5.550	5.500	2.050×10^{-1}	6.525×10^{-2}	3.192×10^{-2}
[0.10, 0.15)	[5.7, 6.0)	5.850	5.816	1.653×10^{-1}	5.186×10^{-2}	2.550×10^{-2}
[0.10, 0.15)	[6.0, 6.3)	6.150	6.139	1.593×10^{-1}	3.486×10^{-2}	2.447×10^{-2}
[0.10, 0.15)	[6.3, 6.6)	6.450	6.440	7.560×10^{-2}	2.478×10^{-2}	1.158×10^{-2}
[0.10, 0.15)	[6.6, 6.9)	6.750	6.746	4.070×10^{-2}	1.434×10^{-2}	6.307×10^{-3}
[0.10, 0.15)	[6.9, 7.5)	7.200	7.114	2.932×10^{-2}	1.115×10^{-2}	4.481×10^{-3}
[0.10, 0.15)	[7.5, 8.7)	8.100	7.838	1.941×10^{-2}	7.930×10^{-3}	2.950×10^{-3}
[0.15, 0.20)	[4.5, 4.8)	4.650	4.656	8.386×10^{-1}	2.133×10^{-1}	1.459×10^{-1}
[0.15, 0.20)	[4.8, 5.1)	4.950	4.920	7.798×10^{-1}	1.766×10^{-1}	1.250×10^{-1}
[0.15, 0.20)	[5.1, 5.4)	5.250	5.251	4.922×10^{-1}	1.046×10^{-1}	7.695×10^{-2}
[0.15, 0.20)	[5.4, 5.7)	5.550	5.520	2.781×10^{-1}	6.083×10^{-2}	4.283×10^{-2}
[0.15, 0.20)	[5.7, 6.0)	5.850	5.833	2.396×10^{-1}	5.007×10^{-2}	3.676×10^{-2}
[0.15, 0.20)	[6.0, 6.3)	6.150	6.138	1.352×10^{-1}	3.967×10^{-2}	2.065×10^{-2}
[0.15, 0.20)	[6.3, 6.6)	6.450	6.467	7.119×10^{-2}	2.568×10^{-2}	1.084×10^{-2}
[0.15, 0.20)	[6.6, 6.9)	6.750	6.748	5.584×10^{-2}	1.640×10^{-2}	8.596×10^{-3}
[0.15, 0.20)	[6.9, 7.5)	7.200	6.919	1.985×10^{-2}	1.594×10^{-2}	3.019×10^{-3}
[0.15, 0.20)	[7.5, 8.7)	8.100	7.632	6.576×10^{-3}	3.945×10^{-3}	1.065×10^{-3}
[0.20, 0.25)	[4.2, 4.5)	4.350	4.347	1.123×10^{0}	3.376×10^{-1}	2.072×10^{-1}
[0.20, 0.25)	[4.5, 4.8)	4.650	4.653	9.809×10^{-1}	2.274×10^{-1}	1.620×10^{-1}
[0.20, 0.25)	[4.8, 5.1)	4.950	4.953	6.905×10^{-1}	1.291×10^{-1}	1.081×10^{-1}
[0.20, 0.25)	[5.1, 5.4)	5.250	5.237	3.602×10^{-1}	7.549×10^{-2}	5.544×10^{-2}

Cont'd on next page

Table 5: (Continued)

x_F Bin	Mass Bin (GeV)	Bin Center (GeV)	Bin Average (GeV)	Cross-Section (nb-GeV^2)	stat. error (nb-GeV^2)	syst. error (nb-GeV^2)
[0.20, 0.25)	[5.4, 5.7)	5.550	5.539	2.830×10^{-1}	5.529×10^{-2}	4.333×10^{-2}
[0.20, 0.25)	[5.7, 6.0)	5.850	5.835	1.885×10^{-1}	3.880×10^{-2}	2.868×10^{-2}
[0.20, 0.25)	[6.0, 6.3)	6.150	6.157	8.814×10^{-2}	3.025×10^{-2}	1.341×10^{-2}
[0.20, 0.25)	[6.3, 6.6)	6.450	6.463	1.114×10^{-1}	2.832×10^{-2}	1.692×10^{-2}
[0.20, 0.25)	[6.6, 6.9)	6.750	6.761	4.295×10^{-2}	1.858×10^{-2}	6.533×10^{-3}
[0.20, 0.25)	[6.9, 7.5)	7.200	7.136	9.224×10^{-3}	1.130×10^{-2}	1.398×10^{-3}
[0.20, 0.25)	[7.5, 8.7)	8.100	7.634	9.030×10^{-3}	3.932×10^{-3}	1.359×10^{-3}
[0.25, 0.30)	[4.2, 4.5)	4.350	4.390	9.555×10^{-1}	2.055×10^{-1}	1.594×10^{-1}
[0.25, 0.30)	[4.5, 4.8)	4.650	4.653	8.799×10^{-1}	1.686×10^{-1}	1.401×10^{-1}
[0.25, 0.30)	[4.8, 5.1)	4.950	4.947	5.381×10^{-1}	9.957×10^{-2}	8.322×10^{-2}
[0.25, 0.30)	[5.1, 5.4)	5.250	5.243	3.692×10^{-1}	6.835×10^{-2}	5.651×10^{-2}
[0.25, 0.30)	[5.4, 5.7)	5.550	5.555	2.607×10^{-1}	5.198×10^{-2}	3.970×10^{-2}
[0.25, 0.30)	[5.7, 6.0)	5.850	5.840	1.580×10^{-1}	3.113×10^{-2}	2.397×10^{-2}
[0.25, 0.30)	[6.0, 6.3)	6.150	6.144	1.193×10^{-1}	2.663×10^{-2}	1.809×10^{-2}
[0.25, 0.30)	[6.3, 6.6)	6.450	6.466	5.200×10^{-2}	1.901×10^{-2}	7.862×10^{-3}
[0.25, 0.30)	[6.6, 6.9)	6.750	6.755	5.223×10^{-2}	1.888×10^{-2}	7.941×10^{-3}
[0.25, 0.30)	[6.9, 7.5)	7.200	7.107	3.464×10^{-2}	9.170×10^{-3}	5.206×10^{-3}
[0.25, 0.30)	[7.5, 8.7)	8.100	7.598	3.508×10^{-3}	2.544×10^{-3}	5.647×10^{-4}
[0.30, 0.35)	[4.2, 4.5)	4.350	4.355	9.682×10^{-1}	1.855×10^{-1}	1.565×10^{-1}
[0.30, 0.35)	[4.5, 4.8)	4.650	4.665	6.779×10^{-1}	1.236×10^{-1}	1.058×10^{-1}
[0.30, 0.35)	[4.8, 5.1)	4.950	4.947	5.308×10^{-1}	9.068×10^{-2}	8.131×10^{-2}
[0.30, 0.35)	[5.1, 5.4)	5.250	5.249	3.533×10^{-1}	6.288×10^{-2}	5.383×10^{-2}
[0.30, 0.35)	[5.4, 5.7)	5.550	5.542	2.390×10^{-1}	4.623×10^{-2}	3.623×10^{-2}
[0.30, 0.35)	[5.7, 6.0)	5.850	5.844	1.341×10^{-1}	2.975×10^{-2}	2.032×10^{-2}
[0.30, 0.35)	[6.0, 6.3)	6.150	6.133	1.089×10^{-1}	2.213×10^{-2}	1.649×10^{-2}
[0.30, 0.35)	[6.3, 6.6)	6.450	6.384	6.800×10^{-2}	2.056×10^{-2}	1.028×10^{-2}
[0.30, 0.35)	[6.6, 6.9)	6.750	6.741	5.420×10^{-2}	1.360×10^{-2}	8.208×10^{-3}
[0.30, 0.35)	[6.9, 7.5)	7.200	7.045	2.497×10^{-2}	6.858×10^{-3}	3.756×10^{-3}
[0.30, 0.35)	[7.5, 8.7)	8.100	7.919	1.181×10^{-2}	4.331×10^{-3}	1.773×10^{-3}
[0.35, 0.40)	[4.2, 4.5)	4.350	4.337	7.196×10^{-1}	1.297×10^{-1}	1.131×10^{-1}
[0.35, 0.40)	[4.5, 4.8)	4.650	4.640	6.796×10^{-1}	1.152×10^{-1}	1.048×10^{-1}
[0.35, 0.40)	[4.8, 5.1)	4.950	4.943	4.901×10^{-1}	8.446×10^{-2}	7.496×10^{-2}
[0.35, 0.40)	[5.1, 5.4)	5.250	5.238	3.254×10^{-1}	5.543×10^{-2}	4.937×10^{-2}
[0.35, 0.40)	[5.4, 5.7)	5.550	5.515	1.406×10^{-1}	3.281×10^{-2}	2.127×10^{-2}
[0.35, 0.40)	[5.7, 6.0)	5.850	5.832	1.385×10^{-1}	2.843×10^{-2}	2.093×10^{-2}
[0.35, 0.40)	[6.0, 6.3)	6.150	6.125	9.033×10^{-2}	2.093×10^{-2}	1.364×10^{-2}
[0.35, 0.40)	[6.3, 6.6)	6.450	6.446	4.087×10^{-2}	1.947×10^{-2}	6.165×10^{-3}
[0.35, 0.40)	[6.6, 6.9)	6.750	6.727	4.011×10^{-2}	1.084×10^{-2}	6.072×10^{-3}
[0.35, 0.40)	[6.9, 7.5)	7.200	7.175	2.263×10^{-2}	6.209×10^{-3}	3.390×10^{-3}
[0.35, 0.40)	[7.5, 8.7)	8.100	7.764	9.710×10^{-3}	3.761×10^{-3}	1.469×10^{-3}
[0.40, 0.45)	[4.2, 4.5)	4.350	4.351	6.714×10^{-1}	1.212×10^{-1}	1.047×10^{-1}
[0.40, 0.45)	[4.5, 4.8)	4.650	4.642	5.134×10^{-1}	8.883×10^{-2}	7.874×10^{-2}
[0.40, 0.45)	[4.8, 5.1)	4.950	4.934	3.737×10^{-1}	6.449×10^{-2}	5.678×10^{-2}
[0.40, 0.45)	[5.1, 5.4)	5.250	5.231	2.572×10^{-1}	4.759×10^{-2}	3.901×10^{-2}
[0.40, 0.45)	[5.4, 5.7)	5.550	5.514	1.904×10^{-1}	3.491×10^{-2}	2.876×10^{-2}
[0.40, 0.45)	[5.7, 6.0)	5.850	5.854	1.021×10^{-1}	2.355×10^{-2}	1.540×10^{-2}
[0.40, 0.45)	[6.0, 6.3)	6.150	6.176	1.010×10^{-1}	2.152×10^{-2}	1.521×10^{-2}

Cont'd on next page

Table 5: (Continued)

x_F Bin	Mass Bin (GeV)	Bin Center (GeV)	Bin Average (GeV)	Cross-Section (nb-GeV^2)	stat. error (nb-GeV^2)	syst. error (nb-GeV^2)
[0.40, 0.45)	[6.3, 6.6)	6.450	6.422	8.200×10^{-2}	1.722×10^{-2}	1.238×10^{-2}
[0.40, 0.45)	[6.6, 6.9)	6.750	6.751	3.902×10^{-2}	9.905×10^{-3}	5.877×10^{-3}
[0.40, 0.45)	[6.9, 7.5)	7.200	7.100	1.729×10^{-2}	8.435×10^{-3}	2.593×10^{-3}
[0.40, 0.45)	[7.5, 8.7)	8.100	7.821	3.316×10^{-3}	4.877×10^{-3}	4.960×10^{-4}
[0.45, 0.50)	[4.2, 4.5)	4.350	4.344	5.316×10^{-1}	9.382×10^{-2}	8.197×10^{-2}
[0.45, 0.50)	[4.5, 4.8)	4.650	4.642	4.566×10^{-1}	7.742×10^{-2}	6.977×10^{-2}
[0.45, 0.50)	[4.8, 5.1)	4.950	4.940	3.634×10^{-1}	6.084×10^{-2}	5.521×10^{-2}
[0.45, 0.50)	[5.1, 5.4)	5.250	5.238	1.934×10^{-1}	3.633×10^{-2}	2.925×10^{-2}
[0.45, 0.50)	[5.4, 5.7)	5.550	5.523	1.407×10^{-1}	2.747×10^{-2}	2.124×10^{-2}
[0.45, 0.50)	[5.7, 6.0)	5.850	5.841	1.047×10^{-1}	2.125×10^{-2}	1.577×10^{-2}
[0.45, 0.50)	[6.0, 6.3)	6.150	6.135	7.260×10^{-2}	1.647×10^{-2}	1.095×10^{-2}
[0.45, 0.50)	[6.3, 6.6)	6.450	6.437	7.758×10^{-2}	1.612×10^{-2}	1.169×10^{-2}
[0.45, 0.50)	[6.6, 6.9)	6.750	6.741	2.839×10^{-2}	8.681×10^{-3}	4.303×10^{-3}
[0.45, 0.50)	[6.9, 7.5)	7.200	7.198	2.889×10^{-2}	7.053×10^{-3}	4.319×10^{-3}
[0.45, 0.50)	[7.5, 8.7)	8.100	7.828	6.752×10^{-3}	2.599×10^{-3}	1.011×10^{-3}
[0.50, 0.55)	[4.2, 4.5)	4.350	4.353	6.177×10^{-1}	1.029×10^{-1}	9.501×10^{-2}
[0.50, 0.55)	[4.5, 4.8)	4.650	4.620	2.623×10^{-1}	4.829×10^{-2}	3.987×10^{-2}
[0.50, 0.55)	[4.8, 5.1)	4.950	4.949	2.420×10^{-1}	4.259×10^{-2}	3.665×10^{-2}
[0.50, 0.55)	[5.1, 5.4)	5.250	5.246	1.756×10^{-1}	3.222×10^{-2}	2.653×10^{-2}
[0.50, 0.55)	[5.4, 5.7)	5.550	5.534	1.216×10^{-1}	2.718×10^{-2}	1.835×10^{-2}
[0.50, 0.55)	[5.7, 6.0)	5.850	5.843	7.100×10^{-2}	1.676×10^{-2}	1.069×10^{-2}
[0.50, 0.55)	[6.0, 6.3)	6.150	6.121	4.488×10^{-2}	1.451×10^{-2}	6.773×10^{-3}
[0.50, 0.55)	[6.3, 6.6)	6.450	6.417	4.836×10^{-2}	1.310×10^{-2}	7.288×10^{-3}
[0.50, 0.55)	[6.6, 6.9)	6.750	6.690	2.704×10^{-2}	7.906×10^{-3}	4.094×10^{-3}
[0.50, 0.55)	[6.9, 7.5)	7.200	7.135	1.315×10^{-2}	4.040×10^{-3}	1.970×10^{-3}
[0.50, 0.55)	[7.5, 8.7)	8.100	7.861	8.646×10^{-3}	3.042×10^{-3}	1.294×10^{-3}
[0.55, 0.60)	[4.2, 4.5)	4.350	4.348	3.313×10^{-1}	5.895×10^{-2}	5.075×10^{-2}
[0.55, 0.60)	[4.5, 4.8)	4.650	4.634	3.055×10^{-1}	5.112×10^{-2}	4.644×10^{-2}
[0.55, 0.60)	[4.8, 5.1)	4.950	4.951	2.106×10^{-1}	3.677×10^{-2}	3.194×10^{-2}
[0.55, 0.60)	[5.1, 5.4)	5.250	5.247	1.289×10^{-1}	2.334×10^{-2}	1.945×10^{-2}
[0.55, 0.60)	[5.4, 5.7)	5.550	5.524	7.481×10^{-2}	1.696×10^{-2}	1.129×10^{-2}
[0.55, 0.60)	[5.7, 6.0)	5.850	5.830	5.187×10^{-2}	1.452×10^{-2}	7.810×10^{-3}
[0.55, 0.60)	[6.0, 6.3)	6.150	6.118	2.691×10^{-2}	1.286×10^{-2}	4.048×10^{-3}
[0.55, 0.60)	[6.3, 6.6)	6.450	6.420	2.321×10^{-2}	9.228×10^{-3}	3.497×10^{-3}
[0.55, 0.60)	[6.6, 6.9)	6.750	6.697	2.299×10^{-2}	6.715×10^{-3}	3.468×10^{-3}
[0.55, 0.60)	[6.9, 7.5)	7.200	7.185	1.455×10^{-2}	4.465×10^{-3}	2.181×10^{-3}
[0.55, 0.60)	[7.5, 8.7)	8.100	7.799	3.803×10^{-3}	1.816×10^{-3}	5.711×10^{-4}
[0.60, 0.65)	[4.2, 4.5)	4.350	4.357	2.716×10^{-1}	4.774×10^{-2}	4.162×10^{-2}
[0.60, 0.65)	[4.5, 4.8)	4.650	4.666	1.660×10^{-1}	3.053×10^{-2}	2.521×10^{-2}
[0.60, 0.65)	[4.8, 5.1)	4.950	4.945	1.174×10^{-1}	2.239×10^{-2}	1.777×10^{-2}
[0.60, 0.65)	[5.1, 5.4)	5.250	5.240	7.452×10^{-2}	1.633×10^{-2}	1.125×10^{-2}
[0.60, 0.65)	[5.4, 5.7)	5.550	5.547	4.908×10^{-2}	1.178×10^{-2}	7.396×10^{-3}
[0.60, 0.65)	[5.7, 6.0)	5.850	5.815	4.222×10^{-2}	1.379×10^{-2}	6.364×10^{-3}
[0.60, 0.65)	[6.0, 6.3)	6.150	6.146	3.251×10^{-2}	1.119×10^{-2}	4.898×10^{-3}
[0.60, 0.65)	[6.3, 6.6)	6.450	6.406	2.460×10^{-2}	6.754×10^{-3}	3.707×10^{-3}
[0.60, 0.65)	[6.6, 6.9)	6.750	6.708	1.032×10^{-2}	8.032×10^{-3}	1.554×10^{-3}
[0.60, 0.65)	[6.9, 7.5)	7.200	7.225	7.869×10^{-3}	3.112×10^{-3}	1.181×10^{-3}

Cont'd on next page

Table 5: (Continued)

x_F Bin	Mass Bin (GeV)	Bin Center (GeV)	Bin Average (GeV)	Cross-Section (nb-GeV^2)	stat. error (nb-GeV^2)	syst. error (nb-GeV^2)
[0.60, 0.65)	[7.5, 8.7)	8.100	8.039	2.259×10^{-3}	1.368×10^{-3}	3.421×10^{-4}
[0.65, 0.70)	[4.2, 4.5)	4.350	4.324	1.659×10^{-1}	3.011×10^{-2}	2.538×10^{-2}
[0.65, 0.70)	[4.5, 4.8)	4.650	4.650	1.242×10^{-1}	2.342×10^{-2}	1.888×10^{-2}
[0.65, 0.70)	[4.8, 5.1)	4.950	4.923	6.892×10^{-2}	1.510×10^{-2}	1.043×10^{-2}
[0.65, 0.70)	[5.1, 5.4)	5.250	5.219	5.822×10^{-2}	1.511×10^{-2}	8.798×10^{-3}
[0.65, 0.70)	[5.4, 5.7)	5.550	5.535	5.575×10^{-2}	1.145×10^{-2}	8.419×10^{-3}
[0.65, 0.70)	[5.7, 6.0)	5.850	5.840	3.039×10^{-2}	7.325×10^{-3}	4.586×10^{-3}
[0.65, 0.70)	[6.0, 6.3)	6.150	6.125	1.993×10^{-2}	8.279×10^{-3}	3.006×10^{-3}
[0.65, 0.70)	[6.3, 6.6)	6.450	6.440	5.959×10^{-3}	6.988×10^{-3}	9.048×10^{-4}
[0.65, 0.70)	[6.6, 6.9)	6.750	6.734	1.170×10^{-2}	4.284×10^{-3}	1.768×10^{-3}
[0.65, 0.70)	[6.9, 7.5)	7.200	7.164	1.361×10^{-2}	4.073×10^{-3}	2.049×10^{-3}
[0.65, 0.70)	[7.5, 8.7)	8.100	7.654	3.270×10^{-2}	2.300×10^{-2}	1.774×10^{-2}
[0.70, 0.75)	[4.2, 4.5)	4.350	4.334	1.217×10^{-1}	2.425×10^{-2}	1.866×10^{-2}
[0.70, 0.75)	[4.5, 4.8)	4.650	4.635	9.677×10^{-2}	1.880×10^{-2}	1.473×10^{-2}
[0.70, 0.75)	[4.8, 5.1)	4.950	4.944	6.132×10^{-2}	1.289×10^{-2}	9.293×10^{-3}
[0.70, 0.75)	[5.1, 5.4)	5.250	5.257	3.449×10^{-2}	9.039×10^{-3}	5.230×10^{-3}
[0.70, 0.75)	[5.4, 5.7)	5.550	5.585	1.992×10^{-2}	6.850×10^{-3}	3.015×10^{-3}
[0.70, 0.75)	[5.7, 6.0)	5.850	5.829	1.574×10^{-2}	4.508×10^{-3}	2.393×10^{-3}
[0.70, 0.75)	[6.0, 6.3)	6.150	6.128	1.714×10^{-2}	5.156×10^{-3}	2.644×10^{-3}
[0.70, 0.75)	[6.3, 6.6)	6.450	6.475	1.296×10^{-2}	4.424×10^{-3}	2.072×10^{-3}
[0.75, 0.80)	[4.2, 4.5)	4.350	4.347	8.694×10^{-2}	1.875×10^{-2}	1.337×10^{-2}
[0.75, 0.80)	[4.5, 4.8)	4.650	4.615	1.363×10^{-2}	8.592×10^{-3}	2.076×10^{-3}
[0.75, 0.80)	[4.8, 5.1)	4.950	4.935	1.345×10^{-1}	7.332×10^{-2}	3.052×10^{-2}

12 Appendix: Transverse Momentum Distributions

References

[1] S. D. Drell and T. M. Yan, Phys. Rev. Lett. 25, 316 (1970).

[2] DocDB 11448-v2, https://seaquest-docdb.fnal.gov/cgi-bin/sso/RetrieveFile?docid=11448&filename=eff_mix_corr.pdf&version=2

[3] DocDB 11427, https://seaquest-docdb.fnal.gov/cgi-bin/sso/RetrieveFile?docid=11427&filename=reco_eff_kinematics.pdf&version=1

[4] DocDB 11467-v4, https://seaquest-docdb.fnal.gov/cgi-bin/sso/ShowDocument?docid=11467

[5] DocDB 11322.